NASA Technical Memorandum 81844

A Simple Method for Converting Frequency-Domain Aerodynamics to the Time Domain

Earl H. Dowell
Langley Research Center
Hampton, Virginia

National Aeronautics
and Space Administration

**Scientific and Technical
Information Branch**

1980

SUMMARY

A simple, direct procedure is developed for converting frequency-domain aerodynamics into indicial aerodynamics. The data required for aerodynamic forces in the frequency domain may be obtained from any available (linear) theory. The method retains flexibility for the analyst and is based upon the particular character of the frequency-domain results. An evaluation of the method is made for incompressible, subsonic, and transonic two-dimensional flows.

INTRODUCTION

For many years, unsteady aerodynamic theories and applications have focused primarily on the frequency domain since the aerodynamic calculation is simplified if the motion of an airfoil or lifting surface is restricted to be simple harmonic (refs. 1 and 2). However, for applications to aeroelastic systems with feedback control and for aeroelastic systems with structural nonlinearities, it is of considerable value to represent the aerodynamic forces in the time domain.

For an aerodynamic theory which is linear in the motion of the aeroelastic system, there is a fundamental correspondence between the frequency and time domains through a Fourier transform pair (refs. 1 to 3). Such a linear theory may still include important physical effects such as shock wave motions in the transonic regime which are sometimes, incorrectly, thought of as being invariably nonlinear. In principle, if the aerodynamic forces are known at a sufficient number of frequencies, a numerical inversion to the time-domain representation is always possible. Such an inversion is rarely practical, however, because the aerodynamic forces are only known at a relatively small number of frequencies. Instead, a parameter identification approach is usually employed whereby time histories of aerodynamic forces are assumed to be sums of exponentials. The time constants and coefficients are chosen to give a best fit to the frequency representation of the aerodynamic forces which has been obtained numerically by some appropriate aerodynamic solution procedure.

Such representations in the time domain date from the early work of Jones (ref. 4) and extend to the recent interesting work of Roger (refs. 5 and 6) and Vepa (ref. 7). Roger employs a particularly straightforward procedure for determining his representations while Vepa uses Padé approximants and a least-squares method. Abel (ref. 8) and Dunn (ref. 9) have subsequently improved upon these methods. It is the purpose here to develop a simple, systematic procedure for time-domain representations which retains flexibility for the analyst and is based upon the particular character of the frequency-domain results. An evaluation of the method is made for incompressible, subsonic, and transonic two-dimensional flows. No difficulty is anticipated in using the method for three-dimensional flows where results are available for the frequency representation of the aerodynamics. Finally, although not emphasized here, the general procedures may be useful when it is desired to convert from time-domain representations to frequency-domain representations. Such applications might arise when

finite-difference aerodynamic calculations lead directly to time-domain results (ref. 10). Marc H. Williams, of Princeton University, provided the frequency-domain data used in the compressible-flow examples.

SYMBOLS

a_i	coefficients of exponential time representation
b	airfoil half-chord
b_i	exponents of exponential time representation
C	Theodorsen function
C_L	lift coefficient
$C_{L_{\dot{h}}}$	lift coefficient due to heaving
C_{L_α}	lift coefficient due to pitching
C_M	moment coefficient
$C_{M_{\dot{h}}}$	moment coefficient due to heaving
C_{M_α}	moment coefficient due to pitching
D	denominator in polynomial representation of Theodorsen function
F	real part of Theodorsen function
G	imaginary part of Theodorsen function
h	heaving displacement
I	total number of terms in sum
i	$(-1)^{1/2}$; also, index for summation
k	reduced frequency, $\omega b/U$
L	lift
M	Mach number
N	numerator in polynomial representation of Theodorsen function
t	time
U	free-stream velocity
α	angle of attack; also, angle of pitch

ρ fluid density

τ dimensional time, Ut/b

ϕ Wagner function

ϕ_c, ϕ_{cm} transient aerodynamic functions

ω frequency

Superscript:

PT piston theory

Subscripts.

I imaginary part

R real part

max maximum

A bar over a symbol denotes Fourier transform; a dot over a symbol denotes derivative with respect to time.

BASIC APPROACH

For definiteness, consider some aerodynamic generalized force, say C_L, due to some step change in a motion variable, say $\dot{h}/U$. Thus,

$$\dot{h}/U = 1 \qquad (\tau > 0) \qquad (1a)$$

$$\dot{h}/U = 0 \qquad (\tau < 0) \qquad (1b)$$

Assume C_L may be represented by

$$C_L = \sum_{i=1}^{I} a_i e^{b_i \tau} \qquad (\tau > 0) \qquad (2a)$$

$$C_L = 0 \qquad (\tau < 0) \qquad (2b)$$

where the a_i, b_i are yet to be determined but it is anticipated that $b_i < 0$. Taking the Fourier transform of equations (1) and (2),

$$\frac{\bar{C}_L}{\bar{h}/U} = \sum_{i=1}^{I} \frac{ika_i}{(-b_i + ik)} \tag{3}$$

where a bar above a quantity denotes Fourier transform and k is the transform variable. Taking the real and imaginary parts of equation (3),

$$\frac{\left(\bar{C}_L\right)_R}{\bar{h}/U} = \sum_{i=1}^{I} \frac{a_i k^2}{b_i^2 + k^2} \tag{4a}$$

$$\frac{\left(\bar{C}_L\right)_I}{\bar{h}/U} = - \sum_{i=1}^{I} \frac{a_i b_i k}{b_i^2 + k^2} \tag{4b}$$

At this point, there are two important questions:

(1) Is a representation such as equation (3) or equations (4) capable of matching the known behavior to arbitrary accuracy by increasing the number of terms retained in the series? This question is answered in the affirmative by numerical examples and, in the special case of incompressible flow, the analytical results of Desmarais (ref. 11).

(2) How can a_i, b_i be determined conveniently, simply, and unambiguously? Vepa has suggested a (modified) least-squares procedure for determining a_i and b_i. Here a simpler procedure is used. The b_i are determined by the extrema of $\left(\bar{C}_L/\bar{h}\right)_I$; then the a_i are determined by a least-squares fit to the frequency-domain data for $\left(\bar{C}_L/\bar{h}\right)_I$ only, subject to the two constraints that the real part is identically satisfied at $k = 0$ and ∞. The resultant $\left(\bar{C}_L/\bar{h}\right)_R$ is then predicted at intermediate k values. Moreover it is assumed that the b_i, which are the poles of the aerodynamic transfer function (see eq. (3)), are independent of the particular generalized force and motion and are inherent characteristics of the dynamics of the fluid. Vepa anticipated this assumption would be useful but did not pursue it. The procedure is shown in this paper to give good results. Dunn (ref. 9) has adopted this assumption partially by using the same b_i for each distinct type of motion, e g., heave and pitch.

For completeness, Roger's procedure is also briefly described here (refs. 5 and 6). A maximum value of reduced frequency k_{max} is selected which is an upper limit on the frequency range of interest. Next the b_i are chosen as

$$b_i = -\frac{i}{I} k_{max} \qquad (i = 0, 1, 2, 3, \ldots, I)$$

The a_i are then determined by a least-squares procedure using both real and imaginary parts of the aerodynamic transfer functions (matrix elements). Another characteristic of Roger's procedure, though not absolutely essential, is that the procedure is applied to the aerodynamic influence matrix relating pressure to downwash, rather than to the matrix relating generalized forces to generalized coordinates. This automatically insures all motions and resultant aerodynamic forces are treated on a common basis. Finally, the limits $k \to 0$ and $k \to \infty$ are not enforced as constraints in Roger's method. Abel (ref. 8) has modified Roger's method to enforce the constraints at $k = 0$.

From both a theoretical and practical point of view, it is better to select only the imaginary part of the aerodynamic transfer function to construct the representation and to allow the real part to be predicted. From a practical point of view, this approach provides an internal check against: (1) numerical errors in the frequency-domain data and (2) deviations of aerodynamic data from linearity in the motion if they are taken from experiment or finite-difference calculations. From a theoretical point of view, the real and imaginary parts are those associated with a single time-dependent function. Thus, constructing a valid representation of the imaginary part is sufficient to insure a valid representation of the real part. In principle, of course, an alternate approach is to construct the representation using the real part of the aerodynamic transfer function and predict the imaginary part. It will become clear in the following examples, however, why this alternate approach is not the preferred choice.

INCOMPRESSIBLE FLOW

For linear, potential, incompressible, two-dimensional flow, the fluid unsteadiness is characterized in the frequency domain by a single function, the Theodorsen function $C(k)$. It is related to the Wagner function ϕ which is the lift due to a step change in downwash at the airfoil three-quarter chord (usually said to be a step change in angle of attack) through a Fourier transform pair (refs. 1 and 2), i.e.,

$$\phi(\tau) = \frac{1}{2\pi} \int_{-\infty}^{\infty} \frac{C(k)}{ik} e^{ik\tau} \, dk \qquad (5)$$

$$C(k) = ik \int_{-\infty}^{\infty} \phi(\tau) e^{-ik\tau} \, d\tau \tag{6}$$

Following the basic approach, assume that ϕ may be represented by

$$\phi(\tau) = \sum_{i=1}^{I} a_i e^{b_i \tau} \qquad (\tau > 0) \tag{7a}$$

$$\phi(\tau) = 0 \qquad (\tau < 0) \tag{7b}$$

Using equations (6) and (7), the corresponding representation of Theodorsen's function is

$$C(k) = \sum_{i=1}^{I} \frac{ika_i}{(-b_i + ik)} \tag{8}$$

or, in terms of its real and imaginary components $C = F + iG$,

$$F = \sum_{i=1}^{I} \frac{a_i k^2}{b_i^2 + k^2} \tag{9a}$$

$$G = -\sum_{i=1}^{I} \frac{a_i b_i k}{b_i^2 + k^2} \tag{9b}$$

The frequency-domain results for F and G are well known (refs. 1 and 2) and are shown as dashed lines in figure 1. The question is how to determine a_i and b_i. First consider the a_i. As $k \to 0$, $F \to 1$; and as $k \to \infty$, $F \to 1/2$. These limits are well known for any aerodynamic theory, since $k \to 0$ is the

steady-flow limit and $k \to \infty$ is given in general (though not for $M = 0$) by the piston theory (refs. 1 and 2).

Requiring equation (9a) to satisfy these limits means $b_1 = 0$ and $a_1 = F(k=0) = 1$ so that

$$a_1 + a_2 + \ldots = F(k=\infty) = 1/2 \tag{10}$$

Consider now equation (9b) and, for simplicity, let $I = 2$ so that only b_2 remains to be determined. There are various ways this might be done, e.g.:

(1) Collocation, i.e., require b_2 to be such that equation (9a) or (9b) is exactly satisfied at some intermediate k

$$0 < k < \infty$$

(2) Least squares, i.e., require equation (9a) and/or (9b) be satisfied in a least-squares sense

Strictly, this second approach leads in general to a nonlinear equation for the b_i. Vepa (ref. 7) avoids this difficulty by rewriting equation (8) as a ratio of two polynomials:

$$C(k) = \frac{N(ik)}{D(ik)} \tag{11}$$

and then multiplying equation (11) through by D, i.e.,

$$D(ik)C(k) = N(ik) \tag{12}$$

before applying the least-squares procedure to determine the coefficients in the polynominals of N and D. This approach does lead to linear algebraic equations for these coefficients. While the procedure put forward below is no more rigorous fundamentally than that of Vepa, it avoids two objections which might be raised about Vepa's procedure. First, the b_i retain their individual identity and are not lost in complicated expressions for the polynomial coefficients of N and D; second, equation (8), or actually equation (9b), is satisfied in a least-squares sense (to determine a_i) and not the modified equation (12). Satisfying equation (12) in a least-squares sense gives undue weighting to high k values.

The procedure suggested here for determining b_2 is simple. For $I = 2$, since $b_1 = 0$,

$$G = -\frac{a_2 b_2 k}{b_2^2 + k^2} \tag{13}$$

Now $G = 0$ at $k = 0,\infty$ (which eq. (13) already satisfies) and has an extremum at $k = 0.2$. (See fig. 1.) Equation (13) has an extremum, using elementary calculus, at

$$k = \pm b_2 \tag{14}$$

Hence, select $b_2 = -0.2$; the minus sign gives the correct sign of G and also provides a stable aerodynamic system. The corresponding approximants to F and G are shown as solid lines in figure 1 along with their exact counterparts. The agreement is reasonable, though certainly imperfect.

The approximant can be improved by increasing I. The question then becomes how to determine the other b_i. If there were several extrema for G (and they were well separated as is typical for the imaginary parts of aerodynamic generalized forces when multiple peaks occur), then a value of b_i would be selected to be equal to the $-k$ value at each peak. In the present example, however, since no other extrema are present, additional b_i are simply added on either side of -0.2 to improve the approximation. In figure 2, results are shown for $b_1 = 0$, $b_2 = -0.1$, $b_3 = -0.2$, and $b_4 = -0.4$ and in figure 3 for $b_1 = 0$, $b_2 = -0.05$, $b_3 = -0.2$, and $b_4 = 0.6$. Note that the b_i on either side of an extremum are chosen here by inspection and iteration. This simplifies the procedure but presumably incurs some loss of accuracy compared to determining the b_i as part of a least-squares solution procedure. The corresponding a_i were determined, after the b_i were selected, by a least-squares fit to equation (9b) for a selected number of k values subject to the constraints of equation (10). The procedure is standard using Lagrange multipliers to invoke the constraints, and the details are omitted. Up to 27 values of k were used, although 15 gave essentially the same results and as few as 5 gave reasonable results.

The representations of figures 2 and 3 are much improved over those of figure 1, with those of figure 3 being somewhat better than those of figure 2. They could be improved further by increasing I. However, this seems unnecessary; instead, comparisons with alternative representations are considered.

The well-known representation of Jones (refs. 1, 2, and 4) is shown in figure 4. This corresponds to $I = 3$ with $b_1 = 0$, $b_2 = -0.0455$, $b_3 = -0.3$ in the present model, but the a_i were not determined by Jones using a least-squares procedure. Using Jones' values of the b_i and a least-squares procedure to determine the a_i changes the details of the representation, although it is not noticeably improved. (See fig. 5.) Thus, it is concluded that Jones' approximant is less accurate than the present $I = 2$ approximant; the basic reason for this is the number and choice of poles.

In figure 6 the b_i are chosen from Desmarais' continued fraction representation (ref. 11) of Theodorsen's function for $I = 4$ (to be discussed further in following sections). The results are comparable to those shown earlier for $I = 4$, but are not better as far as one can judge. Finally, it should be noted that Vepa (ref. 7) using his more elaborate procedure has also obtained excellent representations of F and G.

The quantity b_i is assumed to be real, although from a mathematical point of view, complex conjugate pairs are permissible. Also, all poles are assumed to be simple ones, e.g., no double poles. Complex and double poles were investigated numerically, but their inclusion gave no noticeable improvement. This result is consistent with Desmarais' continued fraction representation which shows that only simple poles exist along the negative, imaginary k-plane axis to any order of approximation. Also, see the discussion of Edwards in reference 3.

Continued Fraction Representation

Let us now turn to a brief review of the very interesting results of Desmarais (ref. 11) for the support they lend to the admittedly heuristic procedure described above. Desmarais has established the following continued fraction representation of Theodorsen's function:

$$C(k) = 1 + \cfrac{(-1/2)}{1 + \cfrac{1}{i4k + 1 \;-\; \cfrac{3}{1 + \cfrac{3}{i4k + 3 \;-\; \cfrac{5}{1 + \cfrac{5}{i4k + 5 \;-\; \cfrac{}{1 + \ldots}}}}}}}$$

This infinite fraction may be truncated to obtain approximations of various orders, and Desmarais has developed convenient recursion formulas for these. At any order of approximation, C(k) is represented by a ratio of polynomials. All of the poles are along the negative imaginary k-axis (corresponding to negative, real b_i), i.e., the branch cut of Theodorsen's function. The poles become infinitely dense as the order of the approximation is increased. The continued fraction representation converges everywhere in the complex k-plane except along the branch cut. Thus, Theodorsen's function has no poles, except possibly along the branch cut.

The practical significance of the above results is that, although in fact there are no poles of $C(k)$, one may expect to obtain an approximation of any desired accuracy by representing $C(k)$ as a rational function whose poles are all along the negative, imaginary k-axis.

For additional discussion of the continued fraction model, see Desmarais (ref. 11). Even though there is no known counterpart for compressible flow, it is possible a similar situation exists. For subsonic flow, at small k the aerodynamic forces behave very much as for incompressible flow, while for large k the aerodynamic forces will asymptotically approach those of "piston theory." Finally, it is worth mentioning that, for a given number of poles the least-squares procedure may be used to obtain a better match with the true $C(k)$ than the continued fraction representation (ref. 11). This is not to say that the latter is, in general, inferior to the former. Indeed, just the opposite is true, as will be clear to the reader. It is simply to say that for the purpose of providing an accurate representation of $C(k)$ by a ratio of polynomials, a better numerical fit can be obtained using the least-squares procedure than that given by any specific order truncation of the continued fraction representation. It is the fact that the latter may be used to generate a systematic and converging representation of any order, as well as the theoretical support it gives for the least squares method, which underscores its fundamental importance.

Wagner Function

Once the a_i, b_i are known, one has a representation of the Wagner function from equations (7). Results were obtained for the $I = 2$ approximant (of fig. 1) and the better of the two $I = 4$ approximants (of fig. 3). For the $I = 4$ representations whose results are shown in figure 3, the corresponding Wagner function representation is indistinguishable from published results (refs. 1 and 2). By contrast, the $I = 2$ result is somewhat different and it is shown along with the exact result in figure 7. Figure 7 and its compressible counterparts are the ultimate results of the present procedure. The excellent agreement between the $I = 4$ approximant and the exact result is very satisfying.

APPLICATION TO COMPRESSIBLE FLOW

Now let us turn to the effects of compressibility. Two examples will be considered. They are a two-dimensional flat plate at $M = 0.7$ and an NACA 64A006 airfoil at $M = 0.84$. The numerical data are, respectively, from classical aerodynamic theory, which assumes an infinitesimal perturbation about a uniform mean flow, and the transonic aerodynamic theory of Williams (refs. 12 and 13), which considers an infinitesimal dynamic perturbation about a non-uniform mean flow including a shock wave. The shock motion due to the airfoil motion is also taken into account in Williams' theory and is consistently treated as infinitesimal.

Flat Plate at $M = 0.7$

For the flat plate at $M = 0.7$, the lift and moment (about midchord) due to heaving and pitching (about midchord) are considered. Hence, four aerodynamic transfer functions are computed: $C_{L_{\dot{h}/U}}$, C_{L_α}, $C_{M_{\dot{h}/U}}$, and C_{M_α}. These are shown in figures 8, 9, 10, and 11 along with an eight-term (pole) representation using the present method. The b_i were chosen from an examination of the imaginary parts of $C_{L_{\dot{h}/U}}$, C_{L_α}, $C_{M_{\dot{h}/U}}$, and C_{M_α}. In general, it is found that the extrema of the imaginary parts of these functions occur at the same k values. However, they are more distinct for some functions than for others. For example, compare $\left(C_{L_{\dot{h}/U}}\right)_I$ in figure 8(b) to $\left(C_{L_\alpha}\right)_I$ in figure 9(b). The latter actually offers a better definition of the extrema than the former. The b_i are as follows:

$b_1 = 0$

$b_2 = 0.03$

$b_3 = -0.1$ (where imaginary part has one extremum)

$b_4 = -0.3$

$b_5 = -0.8$ (where imaginary part has a near extremum)

$b_6 = -1.2$

$b_7 = -1.75$ (another extremum)

$b_8 = -3.5$

The corresponding a_i are given in table I. The results shown are good representations and no others were studied; however, moderate changes in the b_i values and even a reduction in their total number would probably still lead to satisfactory results. These b_i were, in fact, suggested by the results for the second example, which chronologically were obtained first. It should be noted here that the results for C_{M_α} at high k are even better than indicated as the dominant piston theory term has been subtracted out. See subsequent discussion following the next example.

Using the above results, the aerodynamic indicial functions were computed. These are shown in figures 12 and 13. The definitions of the various aerodynamic terms are:

$\dot{h}/U$ ratio of heaving velocity to free-stream velocity

α angle of pitch

$C_L \equiv L/\rho U^2 b$

$C_M \equiv M/\rho U^2 b^2$

where L and M are dimensional lift and moment, respectively, about midchord and b is the dimensional half-chord. As with the incompressible counterpart, the Wagner function, figures 12 and 13 are the ultimate results of the present method. They are the time histories the experimentalist would measure and the inputs to the aeroelastic analyst's equations of motion. At short times (corresponding to high frequencies) the results are expected to be less accurate, even though at $\tau = 0$ the results are exact because of the enforcement of the piston theory constraint in the frequency domain as $k \to \infty$.

The previously published values (ref. 1) of indicial aerodynamic functions for pitch and moment about the quarter-chord are available in a somewhat different form. For heaving, the nondimensonal lift and moment are defined by

$$\phi_c \equiv \frac{L}{2\pi \frac{\rho U^2}{2}(2b)\frac{\dot{h}}{U}}$$

$$\phi_{cm} \equiv \frac{M}{2\pi \frac{\rho U^2}{2}(2b)^2 \dot{h} U}$$

For pitching, the published results are for a step change in pitching velocity, but zero pitch angle - a mathematically well defined but physically artificial motion. No comparisons were made for this case since comparisons of the results for heaving which are shown in figure 14 were so encouraging. Note that not all of the differences between the present results and those previously published should necessarily be attributed to inaccuracies in the present approach. See Ashley's discussion on pages 347 to 350 of reference 1, as well as the original papers cited in reference 1. Also see Edwards (ref. 14).

Vepa (ref. 7) has made a similar comparison to published results using his procedure for $M = 0.5$. Similar agreement (and differences) were noted.

NACA 64A006 Airfoil at $M = 0.84$

The example of an NACA 64A006 airfoil at $M = 0.84$ motivated the present work and, in fact, was completed first. Hence, it is considered in somewhat more detail, including a study of the effects of number of terms retained in the exponential time-history representation and, also, the number of k values used in the least-squares determination of the coefficients of the exponentials.

A. R. Seebass,[1] of the University of Arizona, has also noted the effectiveness of such representations for transonic aerodynamics.

In figures 15 to 18 the transfer functions are shown along with representations obtained by the present method. Consider figure 15 first. Results are shown for eight and four term representations; and, for the latter, 17 and 28 k values are used for the least-square approximation. These results give an indication of the sensitivity of the method to changes in these parameters. The b_i are the same as those used in the $M = 0.7$ flat-plate example, and the a_i are given in table II.

It is clear from comparing the results of figures 15 to 18 to each other and to the earlier results for $M = 0$ and 0.7 that

(1) More terms are required at the higher M to obtain a good representation.

(2) More terms are required for pitching than heaving motion.

(3) More terms are required for moment than for lift.

These conclusions are intuitive but, nevertheless, important.

Consider in particular the results of figure 18 for moment due to pitching. There is a substantial degradation of the representation at high k values as the number of terms retained in the representation is reduced from eight to four. The effect is exaggerated, however, because in figure 18 (as in fig. 11 for $M = 0.7$) the piston-theory contribution (refs. 1 and 2) which is dominant at high frequencies has been subtracted out. The piston-theory contribution is given by

$$C_M^{PT} = -\left(\frac{4}{3M}\right)\left(\frac{\dot{\alpha}b}{U}\right)$$

For a step change in α, this gives a delta function at $\tau = 0$ which is suppressed in the present presentation of the results. For simple harmonic motion, this gives

$$C_M^{PT} = -\frac{4}{3M} ike^{ik\tau} \qquad (\alpha = e^{ik\tau})$$

which clearly dominates for high k over the residual shown in figure 18.

---

[1] In private communication with the author.

Finally, consider the indicial functions which are displayed in figures 19 to 22. They are shown for both a four-term and eight-term approximation using 28 k values. Comparing these results to those for M = 0.7 (cf. figs. 12 and 13), it is seen the indicial lift behaves in a rather similar fashion. However, the indicial moments are different and generally smaller in magnitude. This fact may explain the relatively greater difficulty of obtaining a good representation of the moments at M = 0.84 compared to M = 0.7. There are, of course, no previously published results to which those of figures 19 to 22 may be compared.

Using his procedure for supersonic and transonic flow, Vepa (ref. 7) maintains "for higher order approximants the poles behaved in an erratic manner, often moving into the right half of the $s[= ik]$ plane." Although Vepa suggested a possible way of overcoming these problems, the present procedure by its nature avoids the difficulty. Roger (ref. 6) has also noted this behavior in his work and chooses the b_j to be negative to avoid the problem. Dunn (ref. 9) allows both a_j and b_j to be determined optimally in a least-squares series but does invoke the constraints that the b_j be negative.

CONCLUDING REMARKS

A simple, direct procedure is suggested for converting frequency-domain aerodynamics into indicial aerodynamics. The time-domain presentation is in the form of a sum of exponentials. Examples for classical incompressible and subsonic, compressible flow suggest that known results can be reproduced accurately. New results are presented for transonic flow based upon Williams' frequency-domain theory (AIAA J., vol. 18, no. 6, June 1980). All examples studied are two-dimensional; however, no difficulty is expected in treating three-dimensional flows where the appropriate frequency-domain aerodynamic representations are available.

Not unexpectedly, it is shown that more terms are required in the representation for (1) higher transonic Mach numbers (though presumably for sufficiently high Mach numbers this trend reverses), (2) pitching compared to heaving motion, and (3) moment compared to lift.

Langley Research Center
National Aeronautics and Space Administration
Hampton, VA 23665
August 14, 1980

REFERENCES

1. Bisplinghoff, Raymond L.; Ashley, Holt; and Halfman, Robert L.: Aeroelasticity. Addison-Wesley Pub. Co., Inc., c.1955.

2. Dowell, Earl H., ed.; Curtiss, Howard C., Jr.; Scanlan, Robert H.; and Sisto, Fernando: A Modern Course in Aeroelasticity. Sijthoff & Noordhoff (Netherlands), 1978.

3. Edwards, John W.: Unsteady Aerodynamic Modeling for Arbitrary Motions. AIAA J., vol. 15, no. 4, Apr. 1977, pp. 593-595.

4. Jones, Robert T.: The Unsteady Lift of a Wing of Finite Aspect Ratio. NACA Rep. 681, 1940.

5. Roger, Kenneth L.; Hodges, Garold E.; and Felt, Larry: Active Flutter Suppression - A Flight Test Demonstration. J. Aircr., vol. 12, no. 6, June 1975, pp. 551-556.

6. Roger, Kenneth L.: Airplane Math Modeling Methods for Active Control Design. Structural Aspects of Active Controls, AGARD-CP-228, 1978, pp. 14-1 - 14-11.

7. Vepa, Ranjan: On the Use of Padé Approximants To Represent Unsteady Aerodynamic Loads for Arbitrarily Small Motions of Wings. AIAA Paper No. 76-17, Jan. 1976.

8. Abel, Irving: An Analytical Technique for Predicting the Characteristics of a Flexible Wing Equipped With an Active Flutter-Suppression System and Comparison With Wind-Tunnel Data. NASA TP-1367, 1979.

9. Dunn, H. J.: An Analytical Technique for Approximating Unsteady Aerodynamics in the Time Domain. NASA TP-1738, 1980.

10. Ballhaus, W. F.; and Goorjian, P. M.: Computation of Unsteady Transonic Flows by the Indicial Method. AIAA J., vol. 16, no. 2, Feb. 1978, pp. 117-124.

11. Desmarais, R.: A Continued Fraction Representation for Theodorsen's Circulation Function. NASA TM-81838, 1980.

12. Williams, M. H.: Unsteady Thin Airfoil Theory for Transonic Flows With Embedded Shocks. AIAA J., vol. 18, no. 6, June 1980.

13. Williams, M. H.: Unsteady Airloads in Supercritical Transonic Flows. AIAA Paper 79-0767, Apr. 1979.

14. Edwards, John. W.: Applications of Laplace Transform Methods to Airfoil Motion and Stability Calculations. Technical Papers on Structures and Materials - AIAA 20th Structures, Structural Dynamics, and Materials Conference, April 1979, pp. 465-481. (Available as AIAA Paper 79-0772.)

TABLE I.- AERODYNAMIC TRANSFER FUNCTIONS FOR

A FLAT PLATE AT M = 0.7

a_i	$C_{L_{\dot{h}/U}}$	C_{L_α}	$C_{M_{\dot{h}/U}}$	C_{M_α}	Poles, b_i
a_1	8.798	8.798	4.41	4.41	0
a_2	-1.3613	-1.0541	-.5378	-1.0241	-.03
a_3	-2.1095	-2.5259	-1.6484	-.1414	-.1
a_4	-3.2864	-1.6087	.0058	-5.2324	-.3
a_5	14.8169	5.2806	-.0369	42.879	-.8
a_6	-29.5748	-3.5559	-5.1654	-102.0212	-1.2
a_7	23.2814	4.493	2.4296	76.5064	-1.75
a_8	-4.8503	-4.1129	.5431	-15.3762	-3.5

TABLE II.- AERODYNAMIC TRANSFER FUNCTIONS FOR

AN NACA 64A006 AIRFOIL AT M = 0.84

a_i	$C_{L_{\dot{h}/U}}$	C_{L_α}	$C_{M_{\dot{h}/U}}$	C_{M_α}	Poles, b_i
Four terms					
a_1	$a_{9.2}$ $b_{9.2}$	9.2	0	0	0
a_2	$a_{-5.8886}$ $b_{-5.9815}$	-4.9091	1.7081	.7379	-.1
a_3	$a_{-.0909}$ $b_{-.5006}$	3.1026	-2.2094	-4.8973	-.8
a_4	$a_{1.5415}$ $b_{2.0442}$	-2.6314	.5012	4.1594	-1.75
Eight terms					
a_1	$a_{9.2}$	9.2	-0.1	-0.1	0
a_2	.5501	1.3655	-.3135	-1.3147	-.03
a_3	-5.1476	-6.384	1.6297	3.0863	-.1
a_4	-2.4487	1.3039	.379	-3.0981	-.3
a_5	5.1096	-17.1412	-.2292	20.9301	-.8
a_6	-7.8209	45.2519	-3.922	-54.9848	-1.2
a_7	7.8616	-34.5566	1.7436	43.1282	-1.75
a_8	-2.5421	5.7225	.8125	-7.6470	-3.5

[a]28 values with $k_{max} = 3.75$.
[b]17 values with $k_{max} = 1.0$.

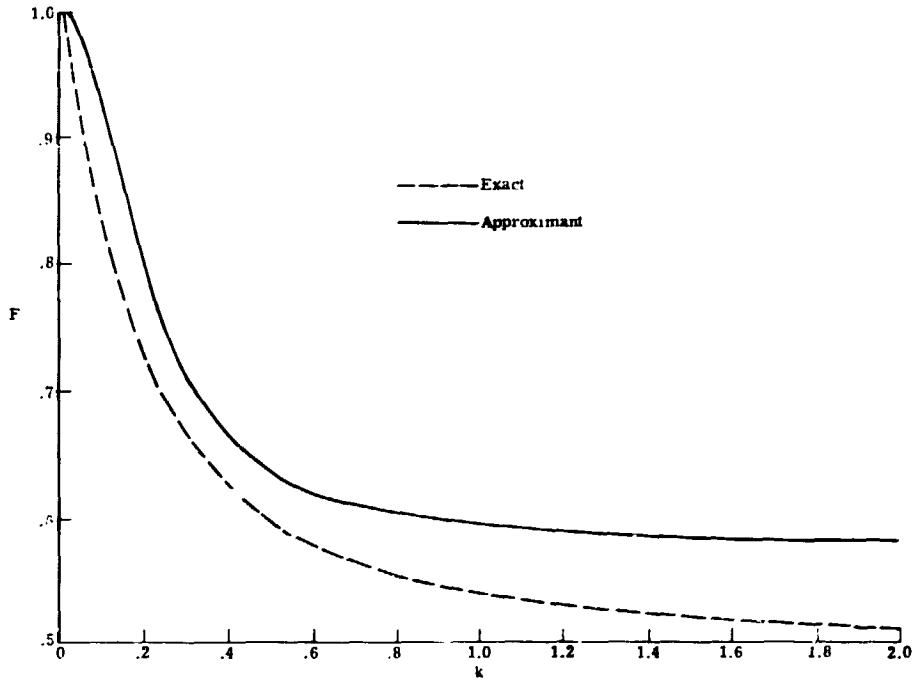

(a) Real part.

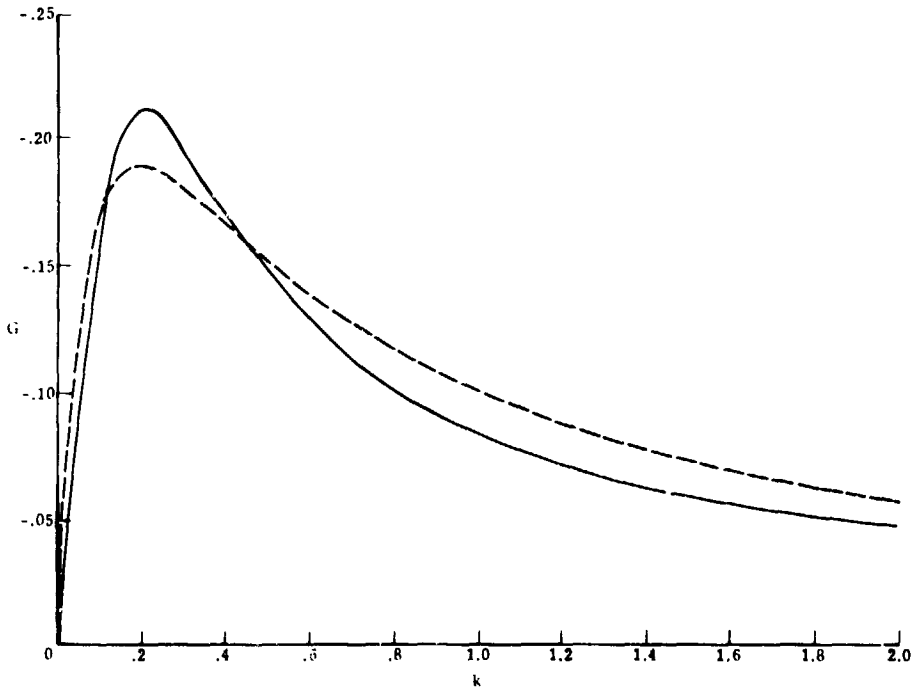

(b) Imaginary part.

Figure 1.- Theodorsen function for $I = 2$, $b_1 = 0$, $b_2 = -0.2$, $a_1 = 1.0$, $a_2 = -0.5$.

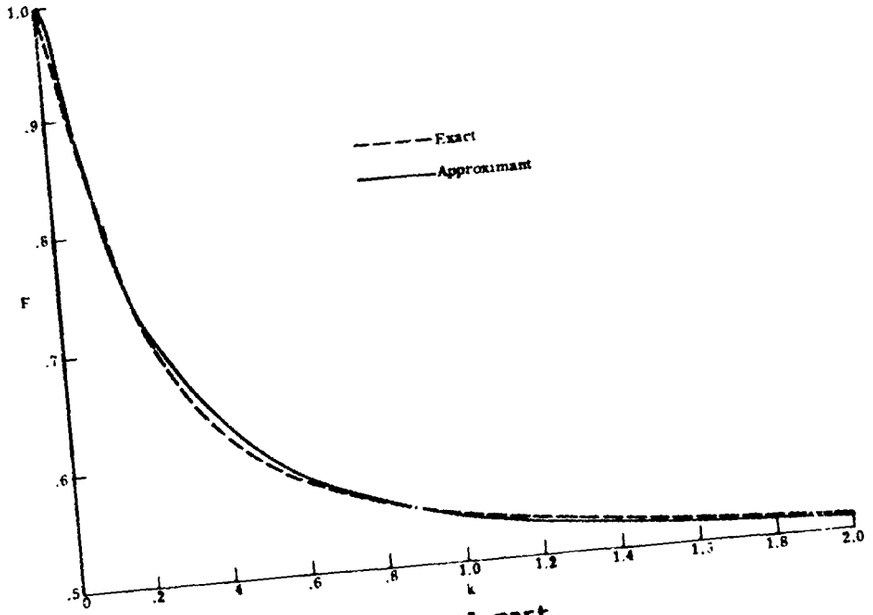

(a) Real part.

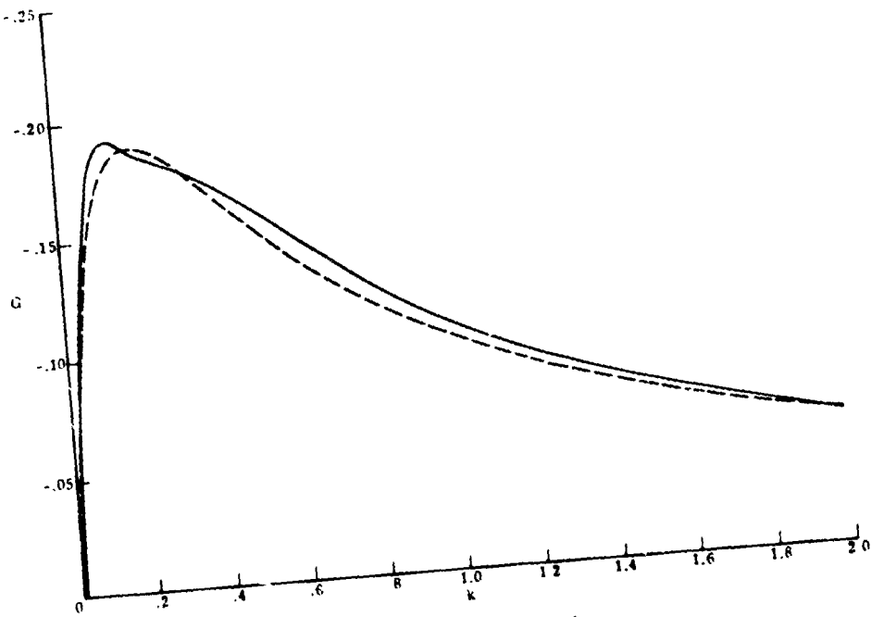

(b) Imaginary part.

Figure 2.- Theodorsen function for $I = 4$, $b_1 = 0$, $b_2 = -0.1$, $b_3 = -0.2$, $b_4 = -0.4$, $a_1 = 1.0$, $a_2 = -0.3576$, $a_3 = 0.1417$, $a_4 = -0.2841$.

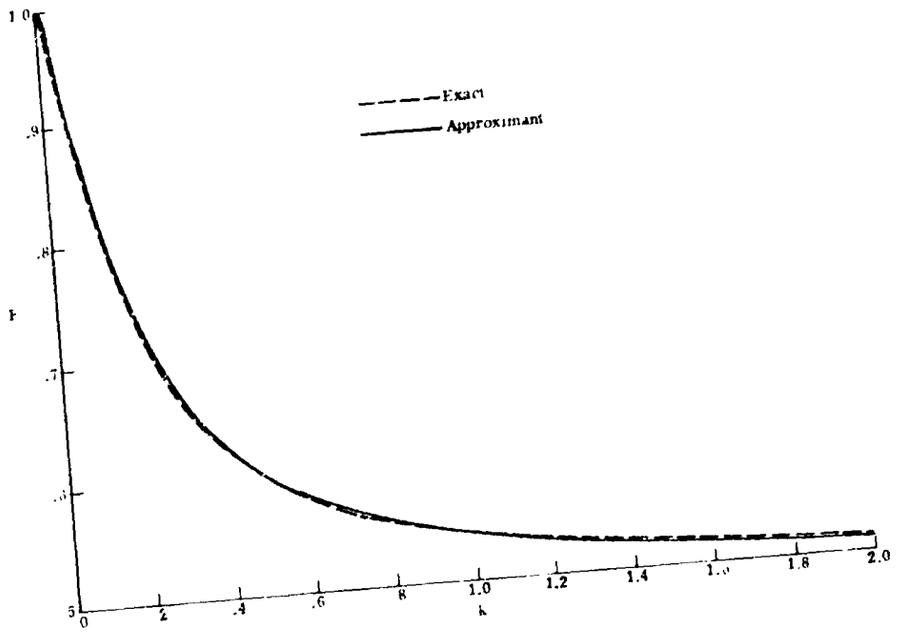

(a) Real part.

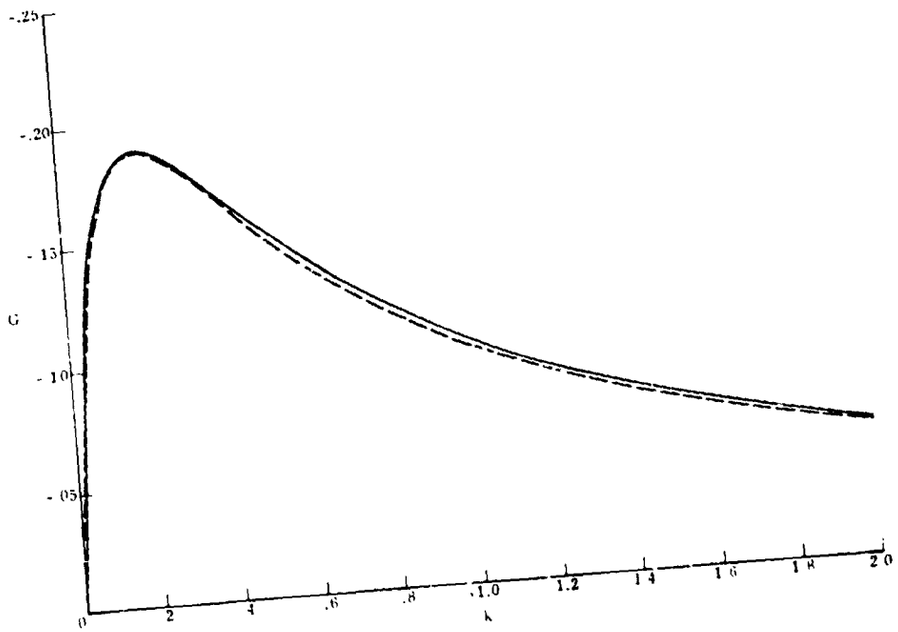

(b) Imaginary part.

Figure 3.- Theodorsen function for $I = 4$, $b_1 = 0$, $b_2 = -0.05$, $b_3 = -0.2$, $b_4 = -0.6$, $a_1 = 1.0$, $a_2 = -0.1465$, $a_3 = -0.2435$, $a_4 = -0.1100$.

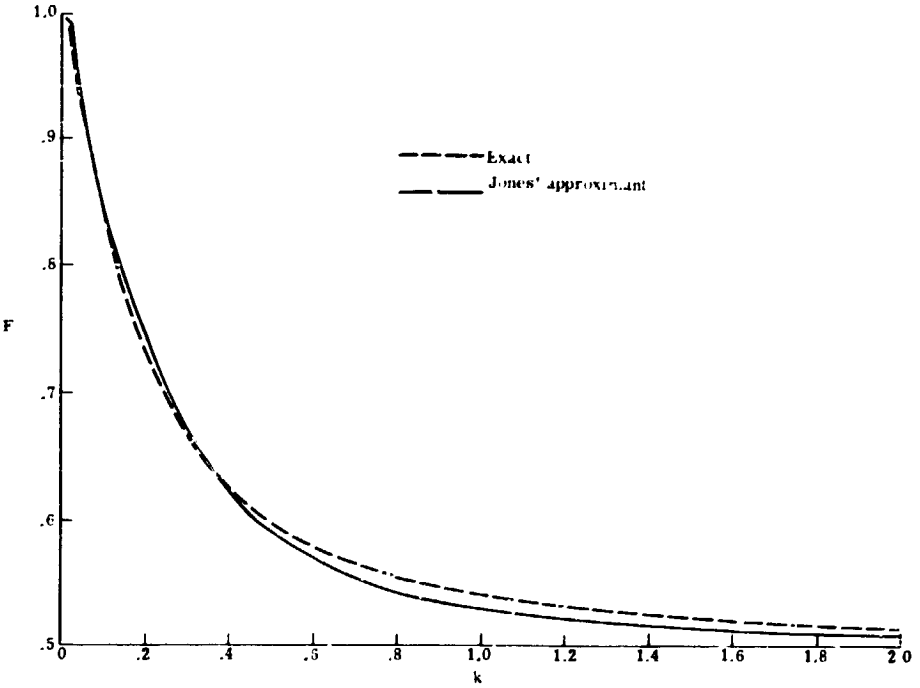

(a) Real part.

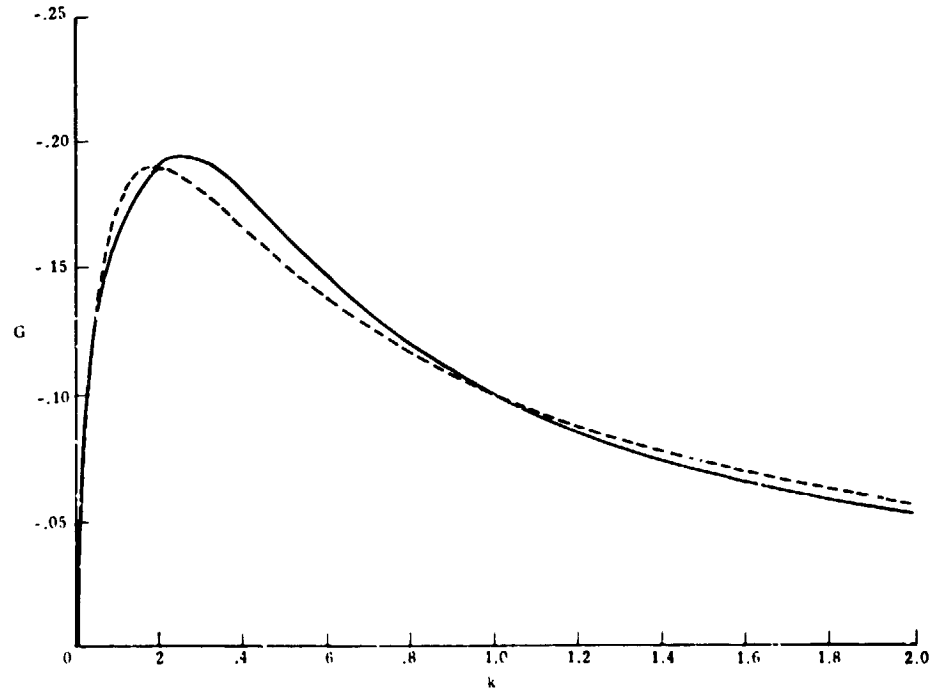

(b) Imaginary part.

Figure 4.- Theodorsen function for $I = 3$, $b_1 = 0$, $b_2 = -0.0455$, $b_3 = -0.3$, $a_1 = 1.0$, $a_2 = -0.165$, $a_3 = -0.335$.

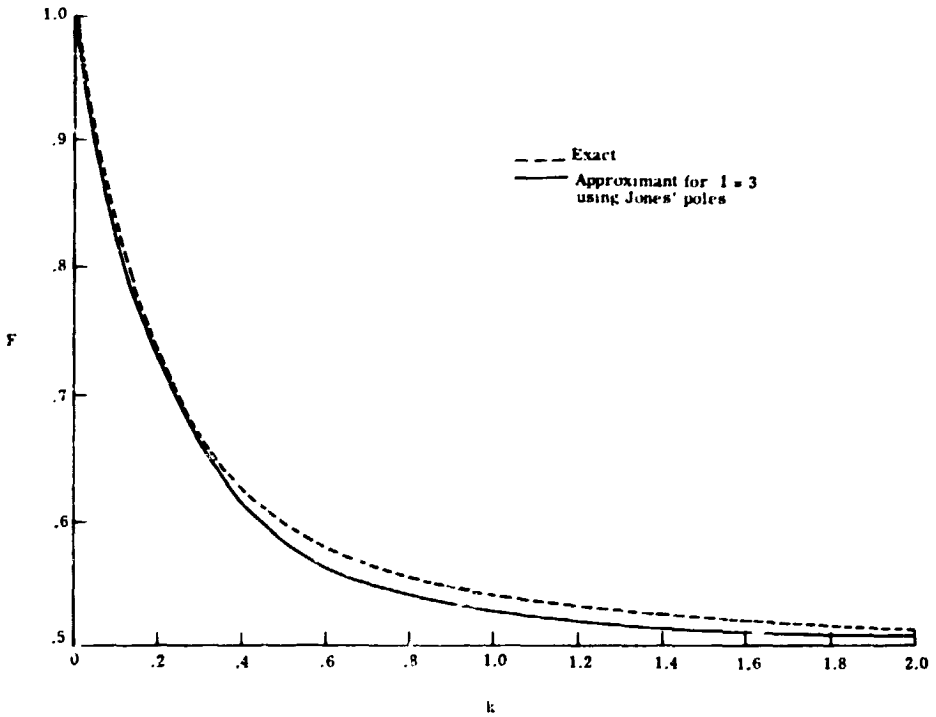

(a) Real part.

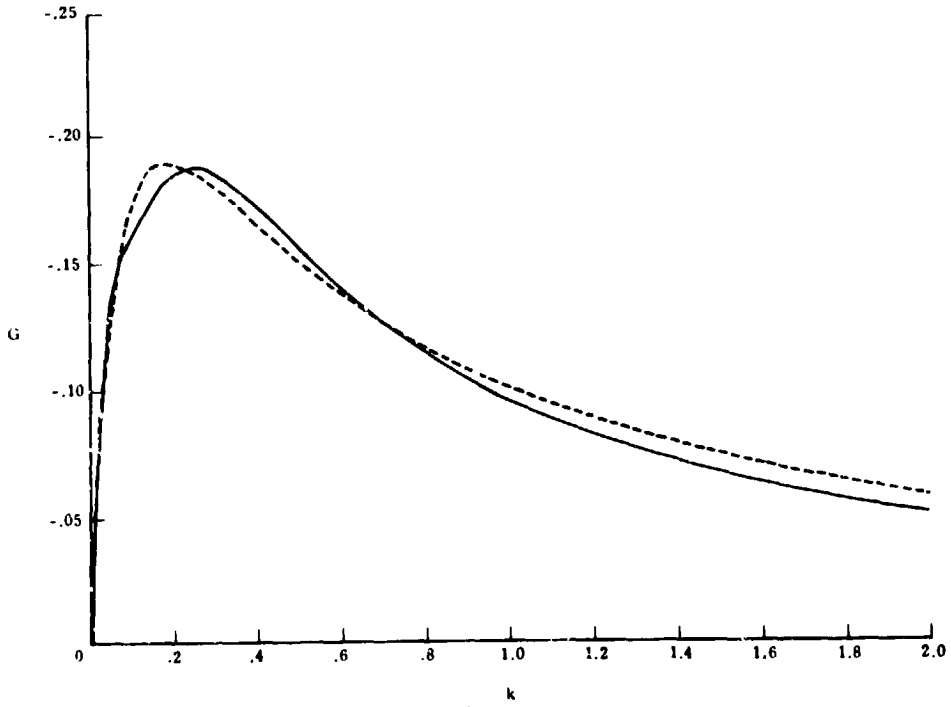

(b) Imaginary part.

Figure 5.- Theodorsen function for $I = 3$, $b_1 = 0$, $b_1 = 0$, $b_2 = -0.0455$, $b_3 = -0.3$, $a_1 = 1.0$, $a_2 = -0.1740$, $a_3 = -0.3166$. (a_i calculated by least-squares procedure.)

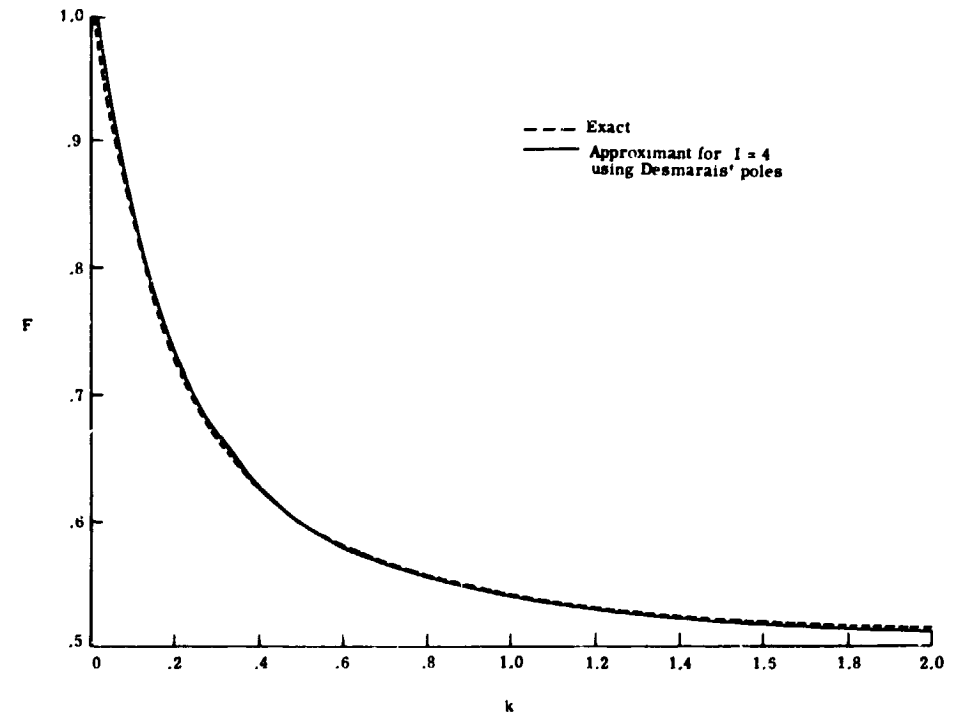

(a) Real part.

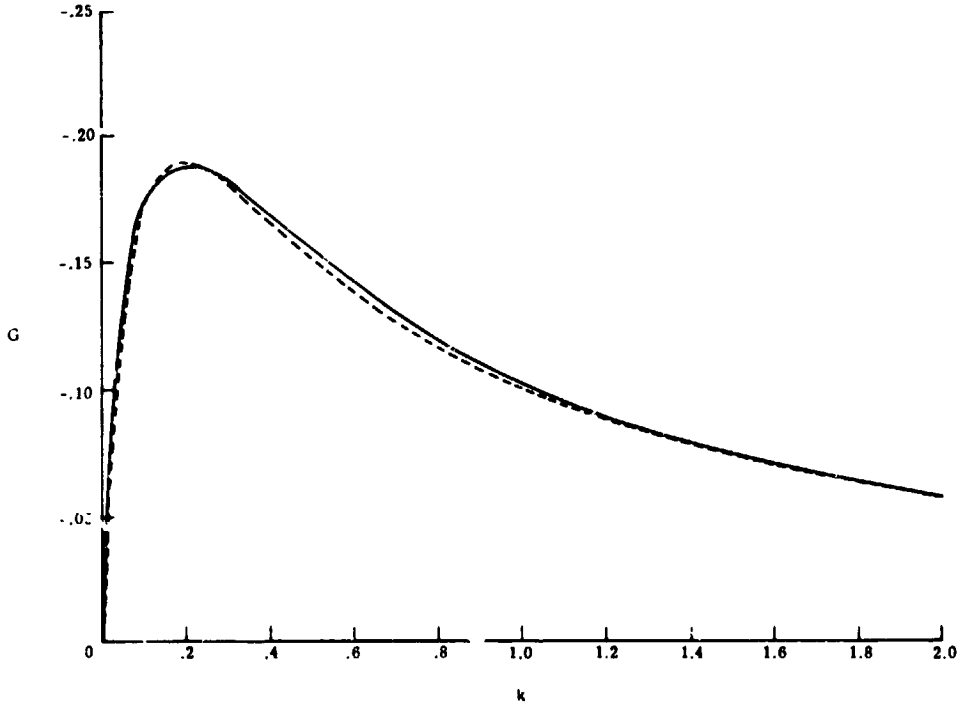

(b) Imaginary part.

Figure 6.- Theodorsen function for $I = 4$, $b_1 = 0$, $b_2 = -0.0594$, $b_3 = -0.2536$, $b_4 = -0.6519$, $a_1 = 1.0$, $a_2 = -0.1873$, $a_3 = -0.2358$, $a_4 = -0.0769$. (a_i calculated by least-squares procedure.)

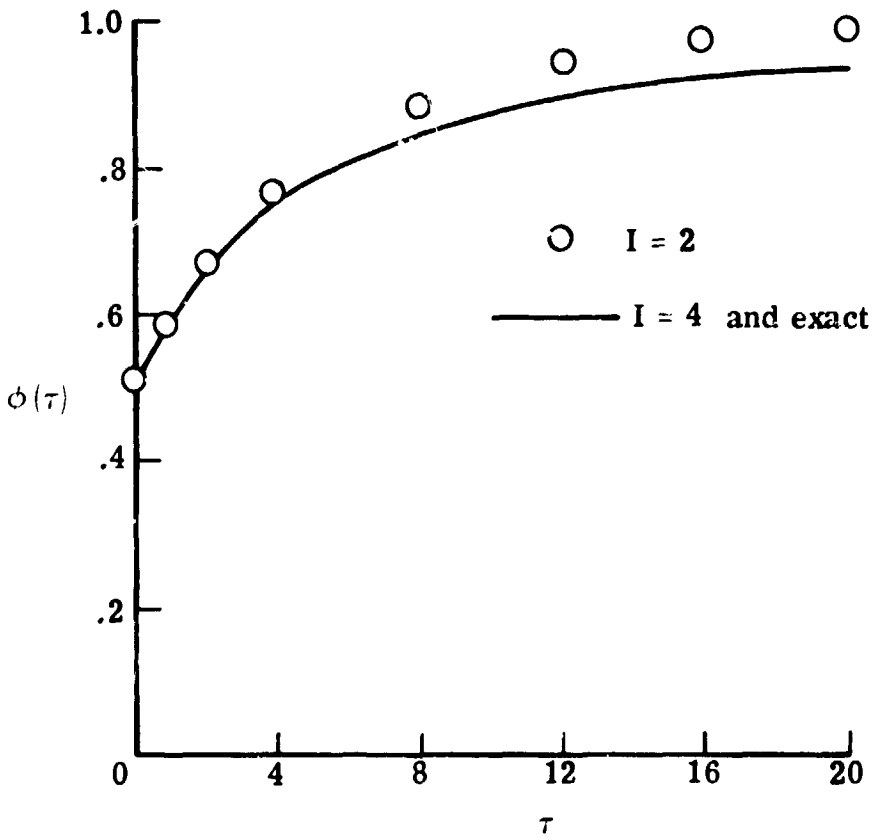

Figure 7.- Wagner function.

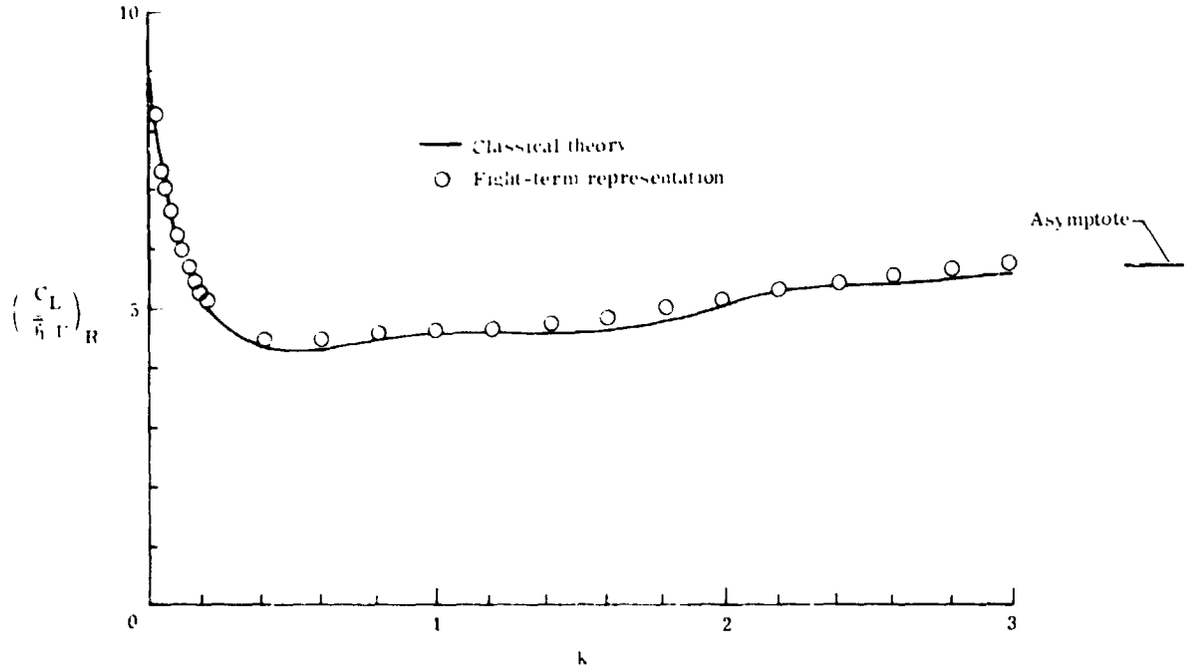

(a) Real part.

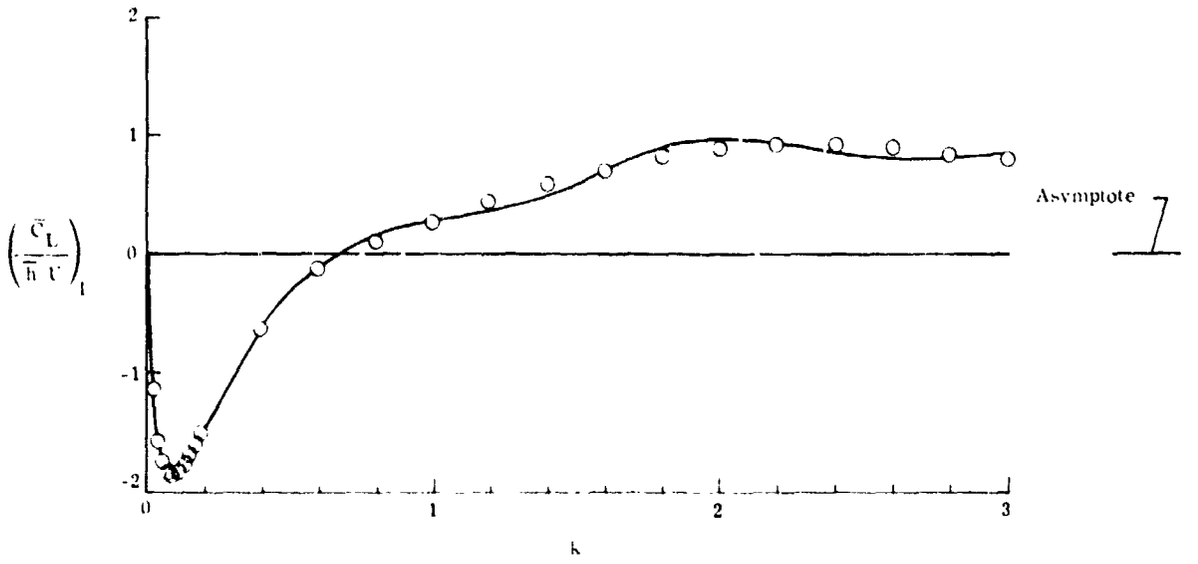

(b) Imaginary part.

Figure 8.- Lift due to heaving for a flat plate at M = 0.7. 25k values, k_{max} = 3.0. (See table I for values of a_i and b_i.)

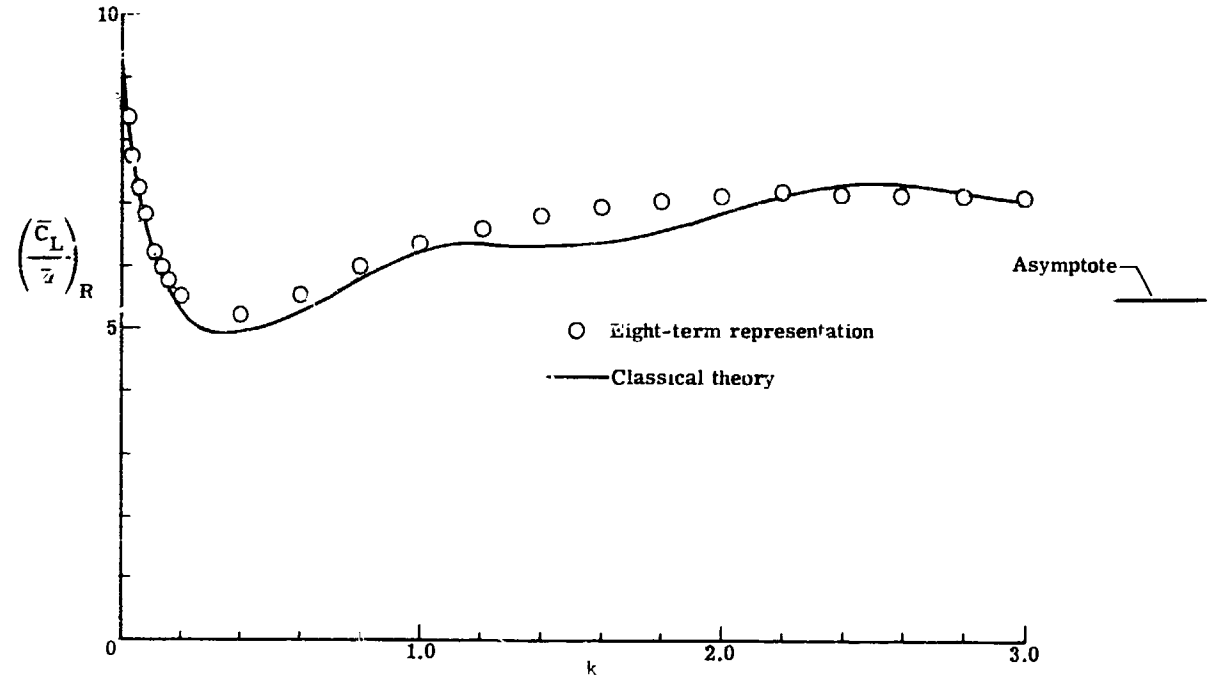

(a) Real part.

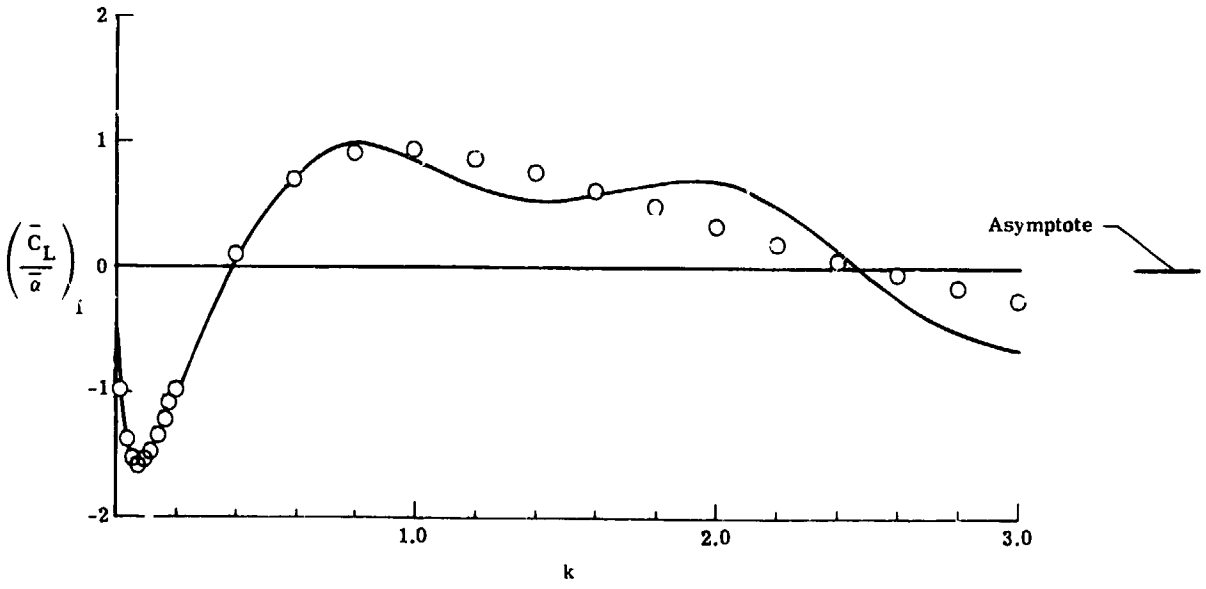

(b) Imaginary part.

Figure 9.- Lift due to pitching for a flat plate at $M = 0.7$. (See table I for values of a_i and b_i.)

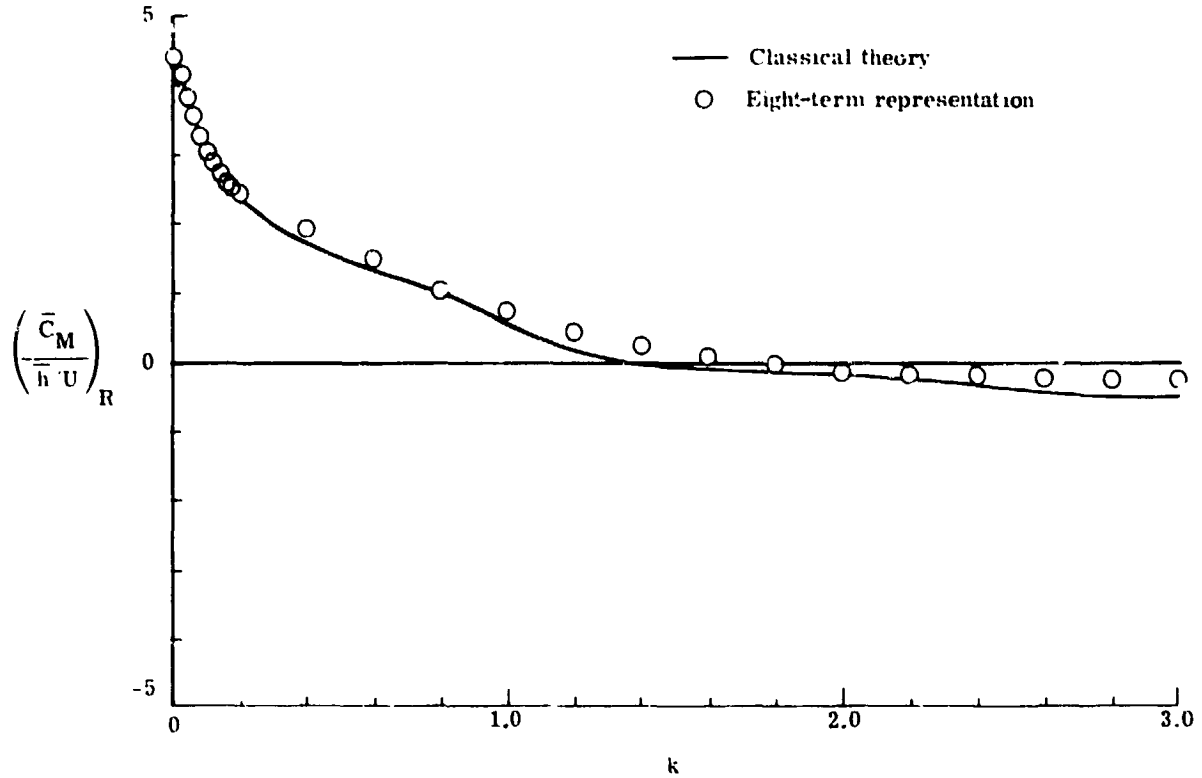

(a) Real part.

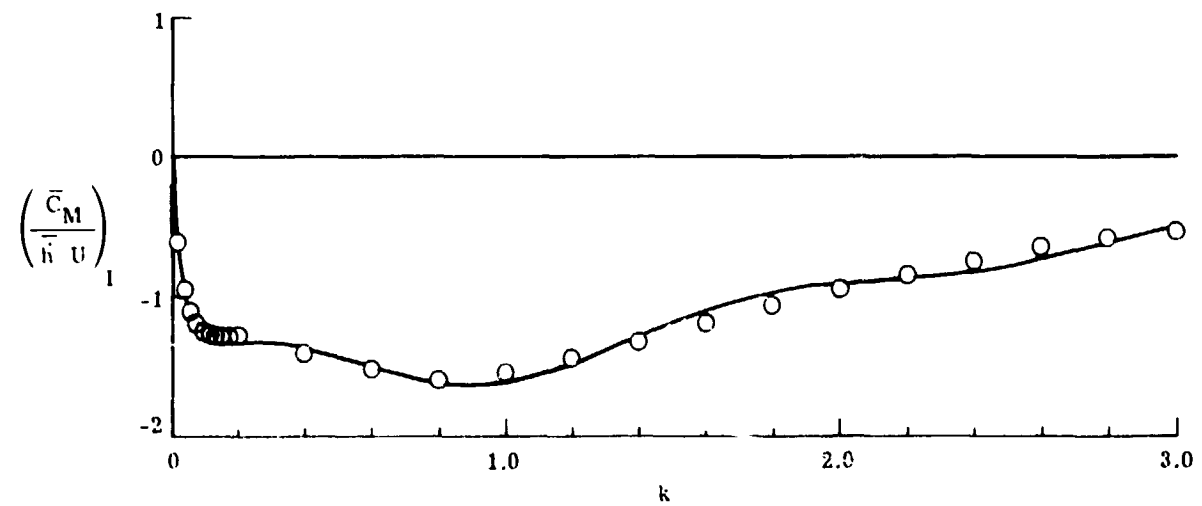

(b) Imaginary part.

Figure 10.- Moment due to heaving for a flat plate at M = 0.7. (See table I for values of a_i and b_i.)

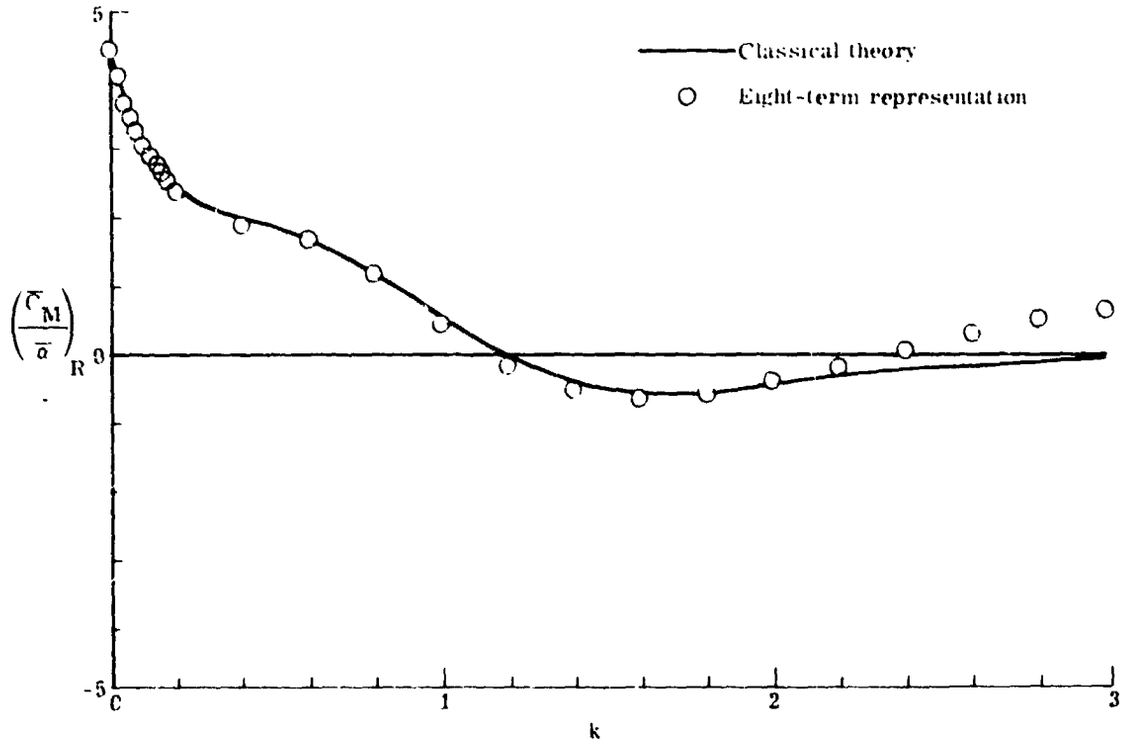

(a) Real part.

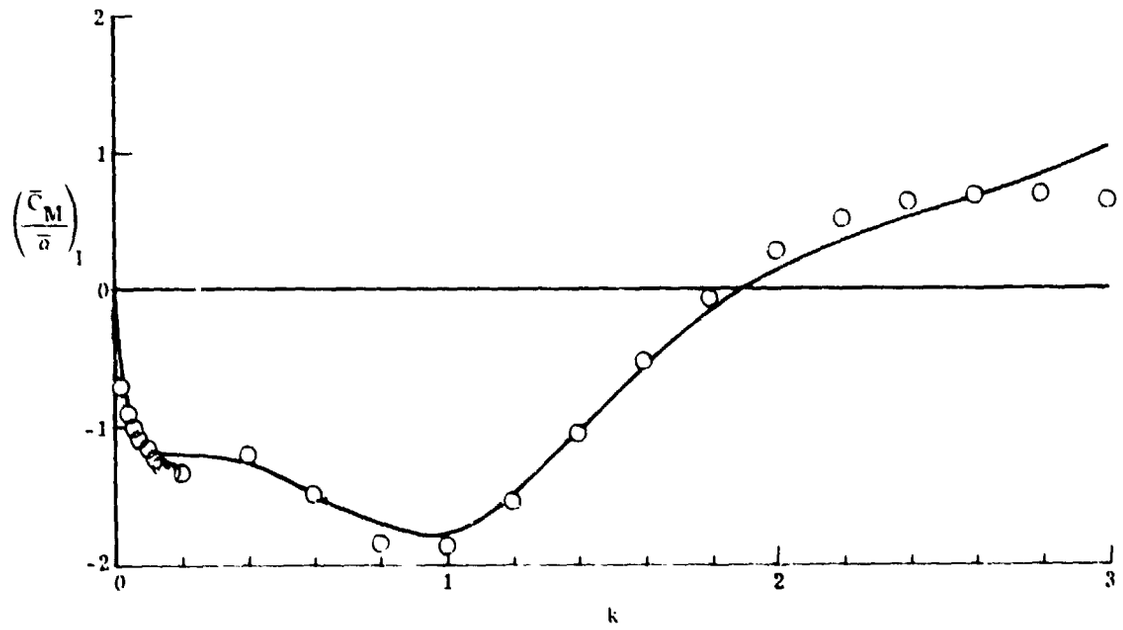

(b) Imaginary part.

Figure 11.- Moment due to pitching for a flat plate at M = 0.7. (See table I for values of a_i and b_i.)

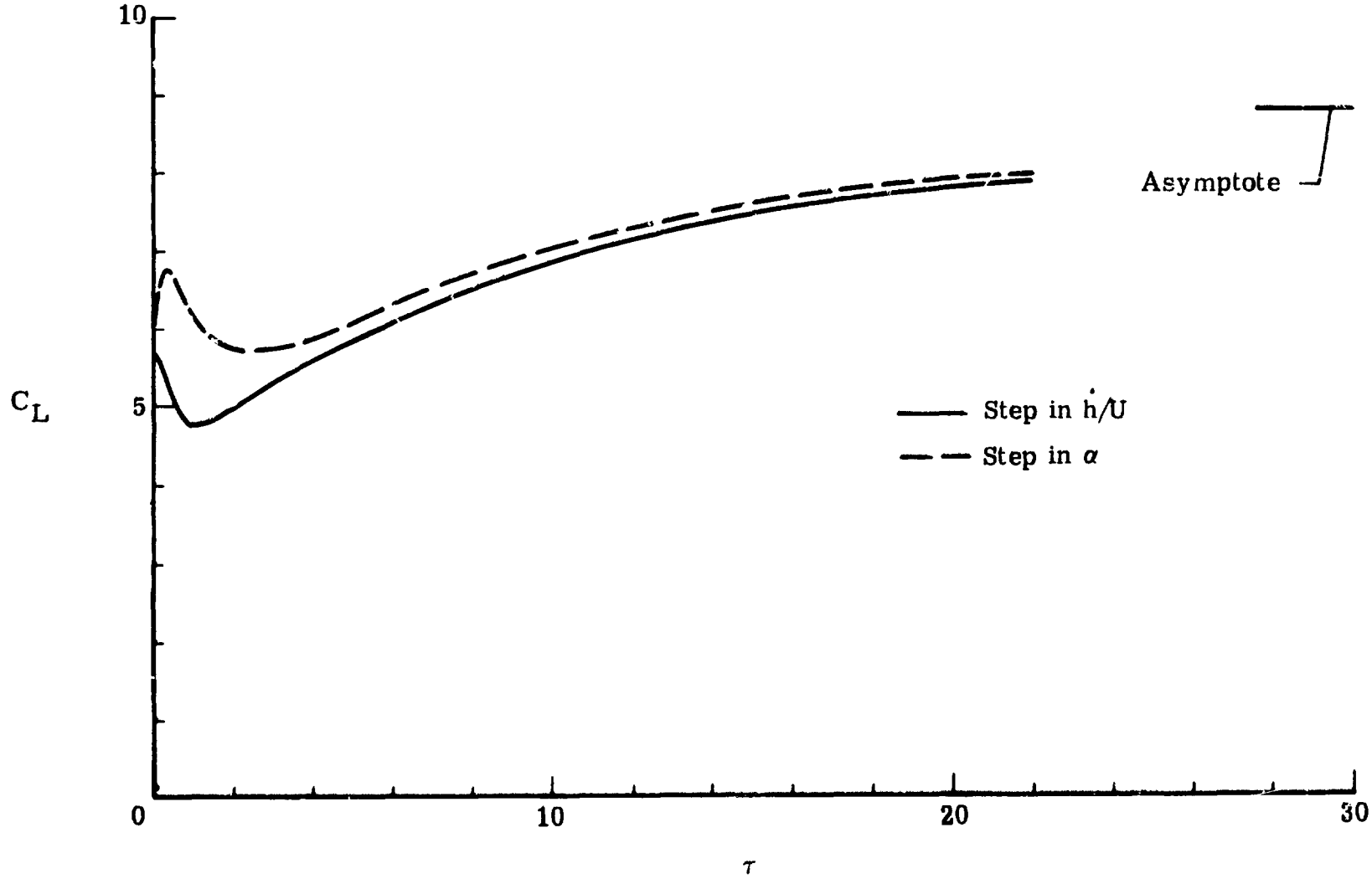

Figure 12.- Indicial lift with eight-term representation. (See table I for values of a_i and b_i.)

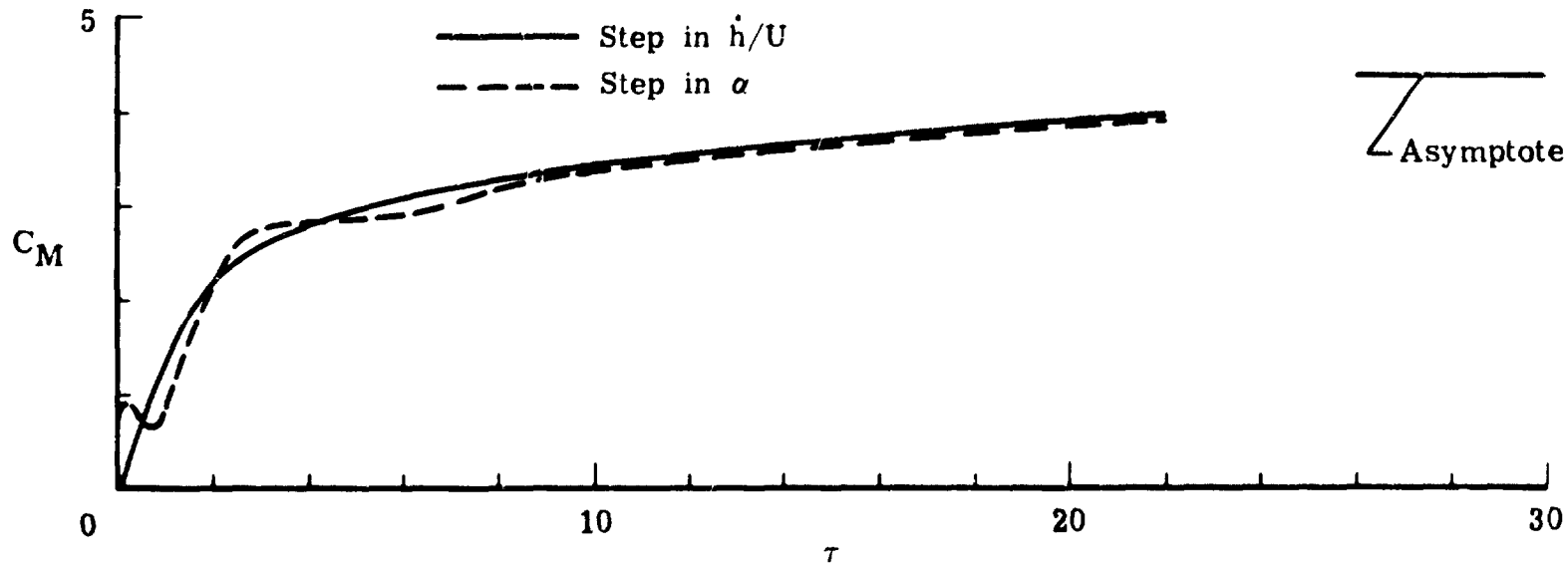

Figure 13.- Indicial moment with eight-term representation. (See table I for values of a_i and b_i.)

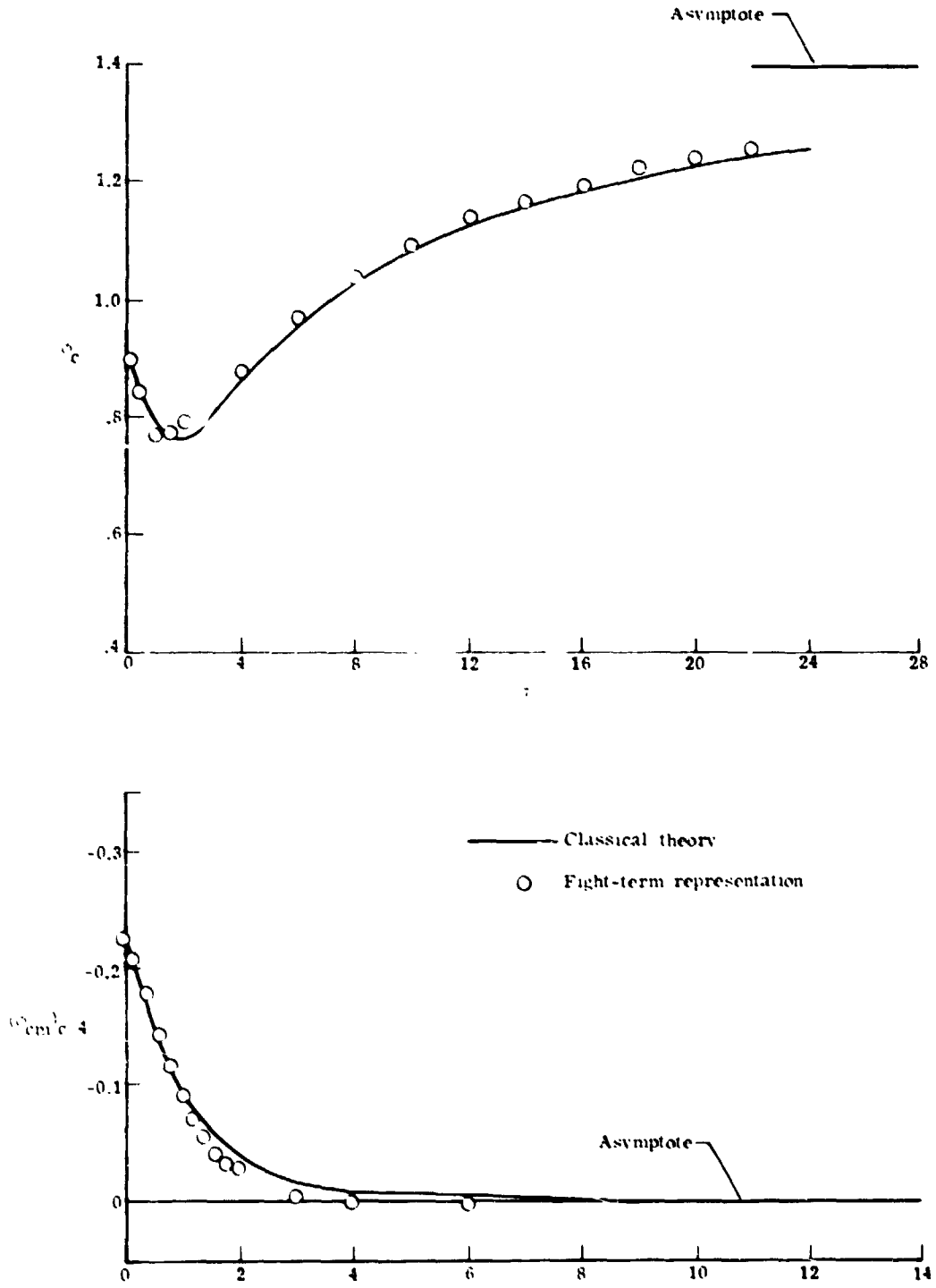

Figure 14.- Indicial lift and moment for heaving of a flat plate at M = 0.7. (See table I for values of a_i and b_i.)

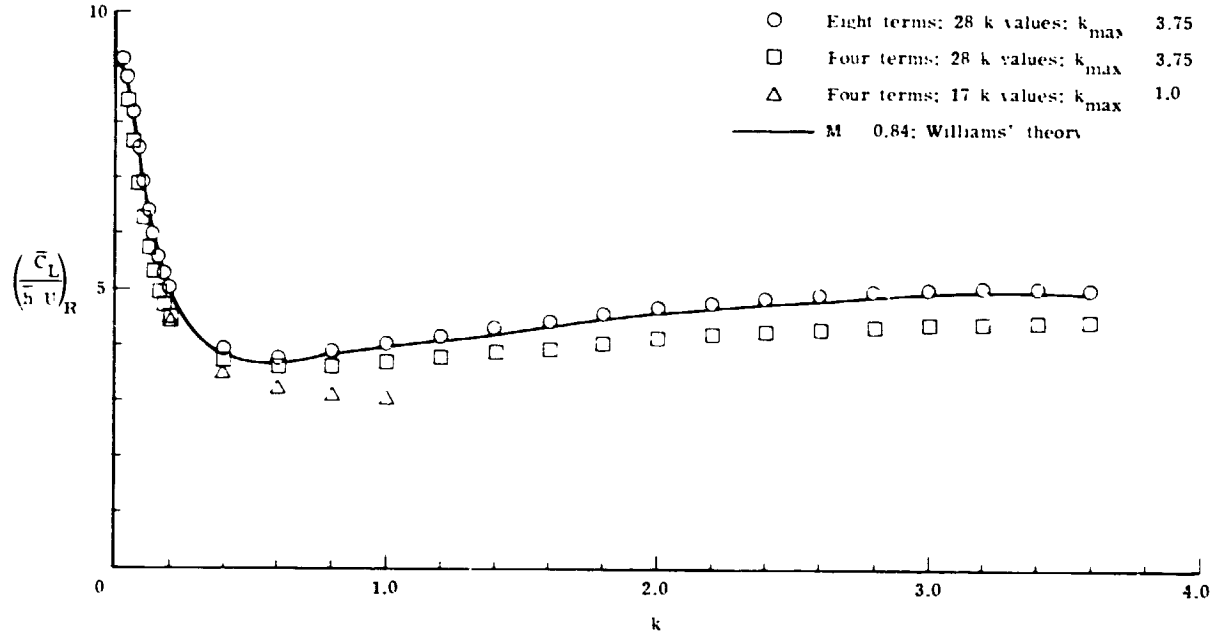

(a) Real part.

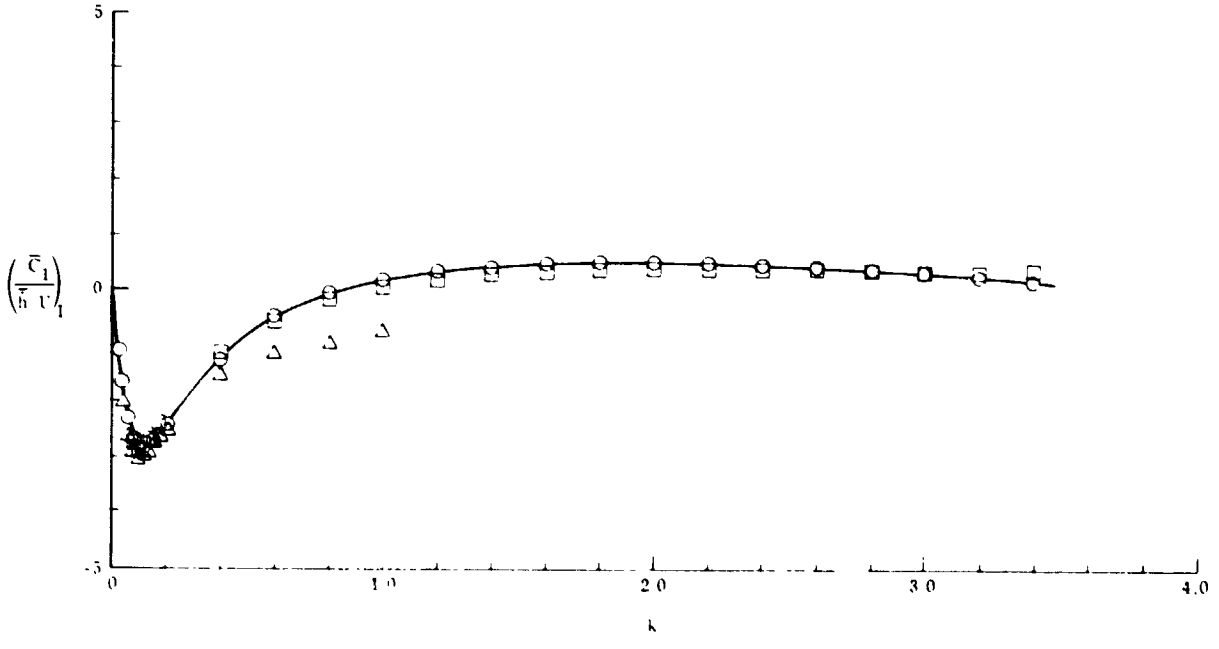

(b) Imaginary part.

Figure 15.- Lift due to heaving for an NACA 64A006 airfoil. (See table II for values of a_i and b_i.)

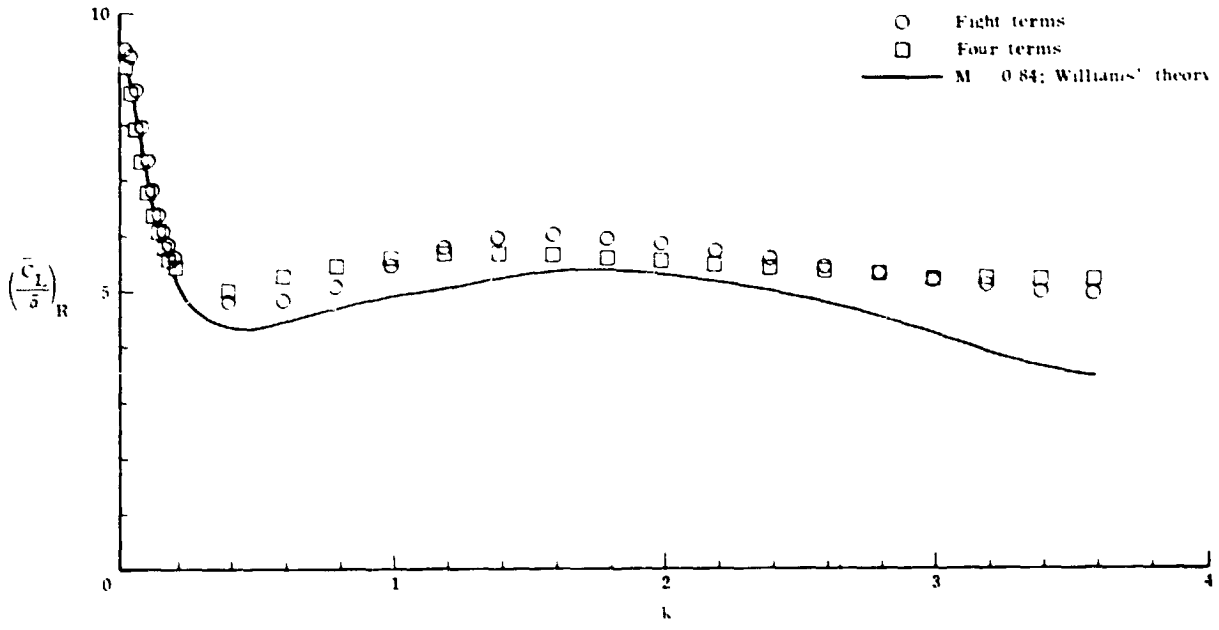

(a) Real part.

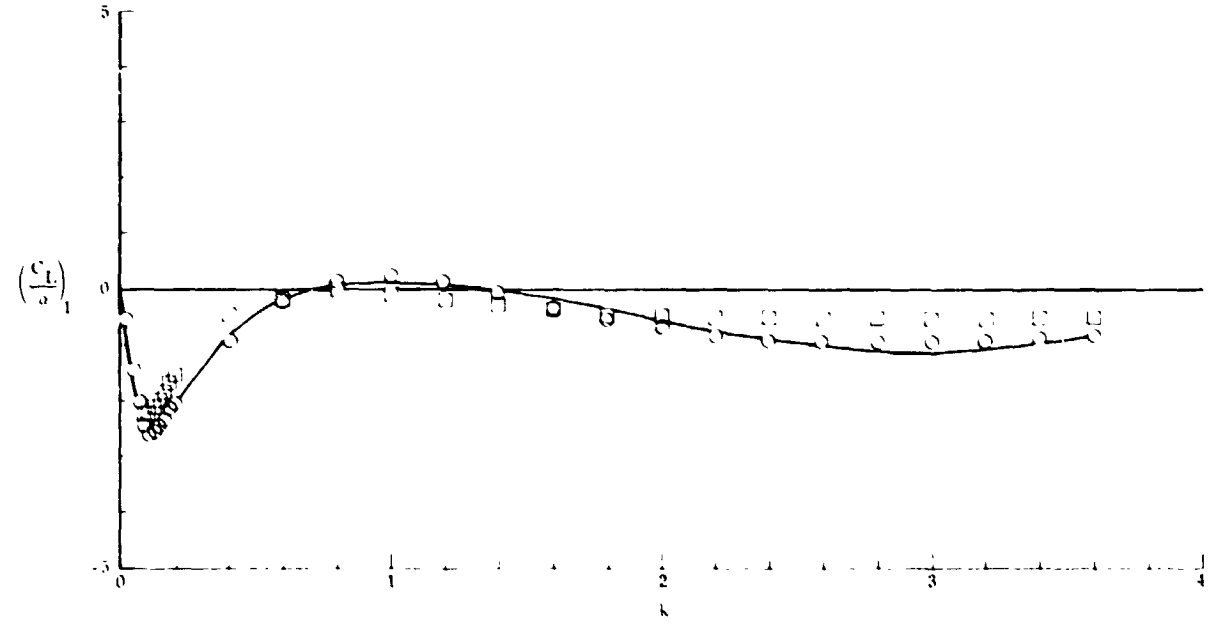

(b) Imaginary part.

Figure 16.- Lift due to pitching for an NACA 64A006 airfoil. (See table II for values of a_i and b_i.)

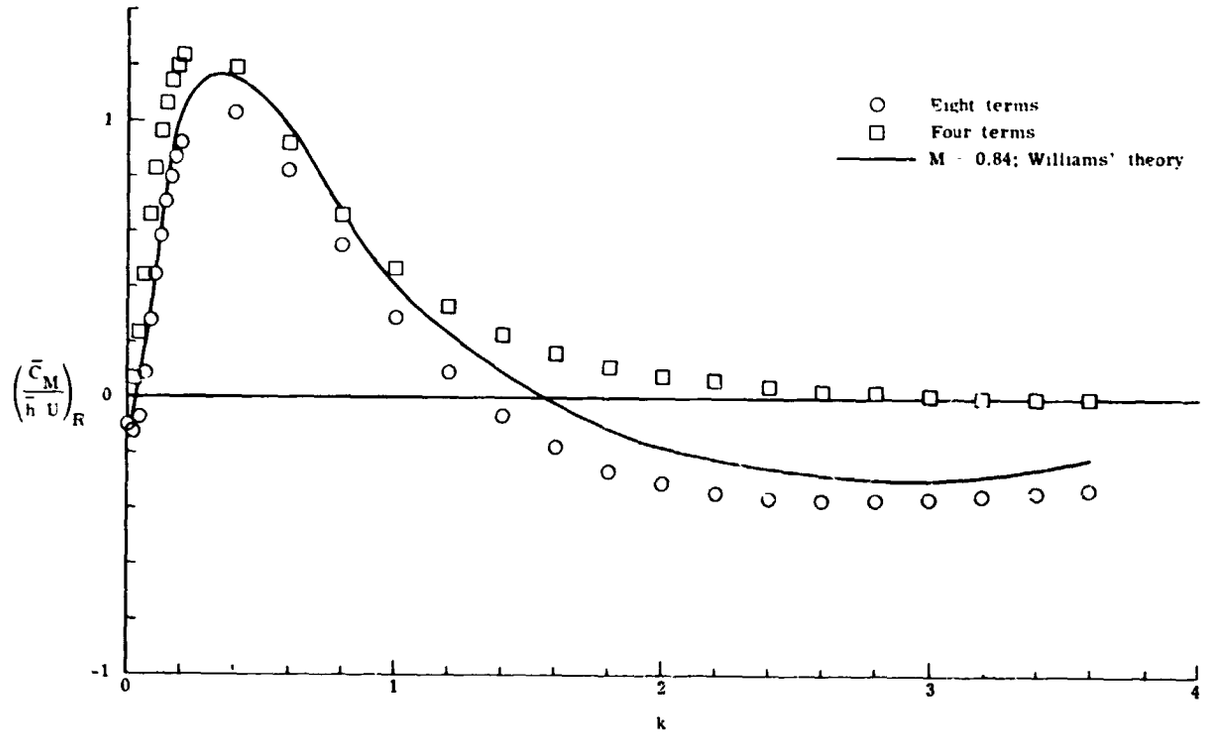

(a) Real part.

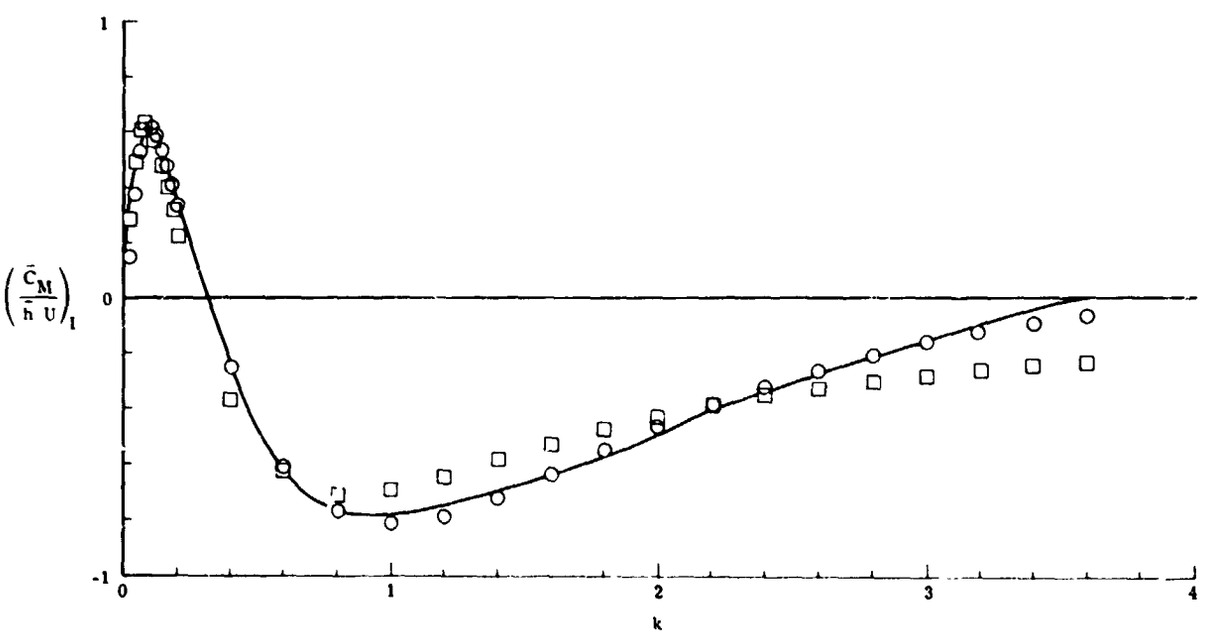

(b) Imaginary part.

Figure 17.- Moment due to heaving for an NACA 64A006 airfoil. (See table II for values of a_i and b_i.)

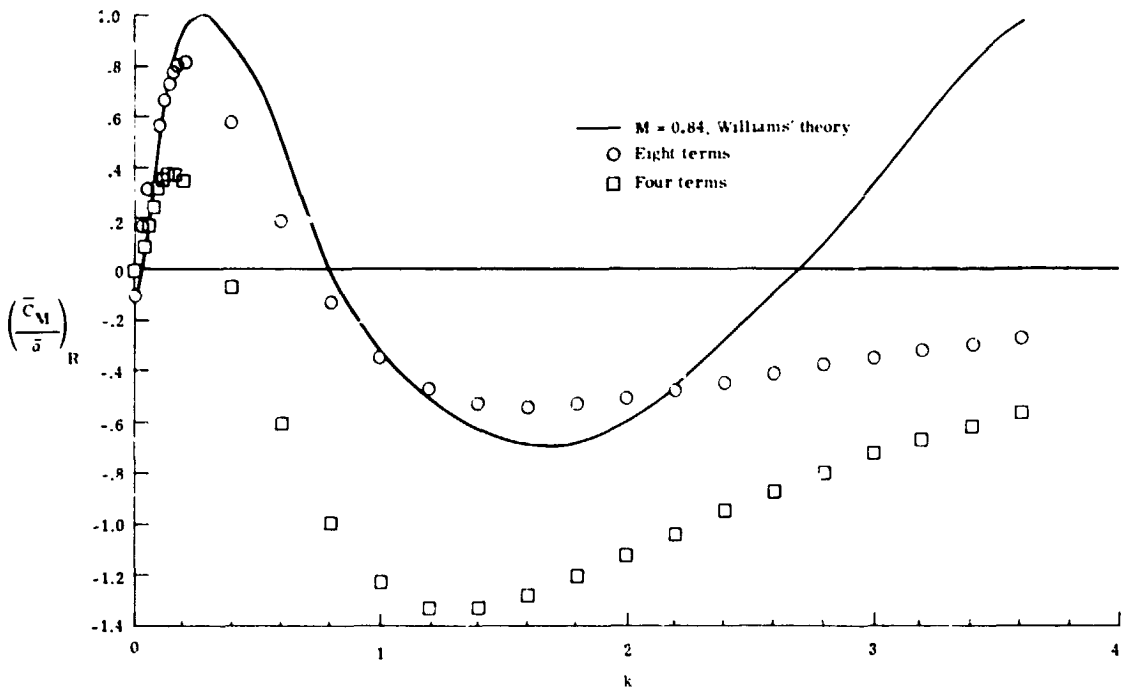

(a) Real part.

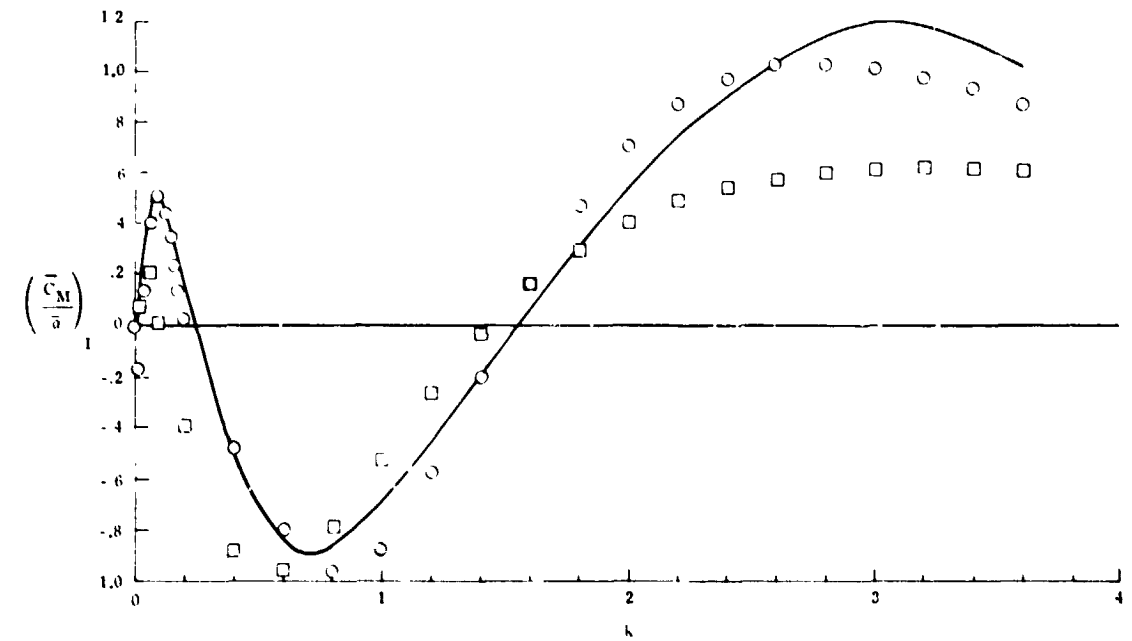

(b) Imaginary part.

Figure 18.- Moment due to pitching for an NACA 64A006 airfoil. (See table II for values of a_i and b_i.)

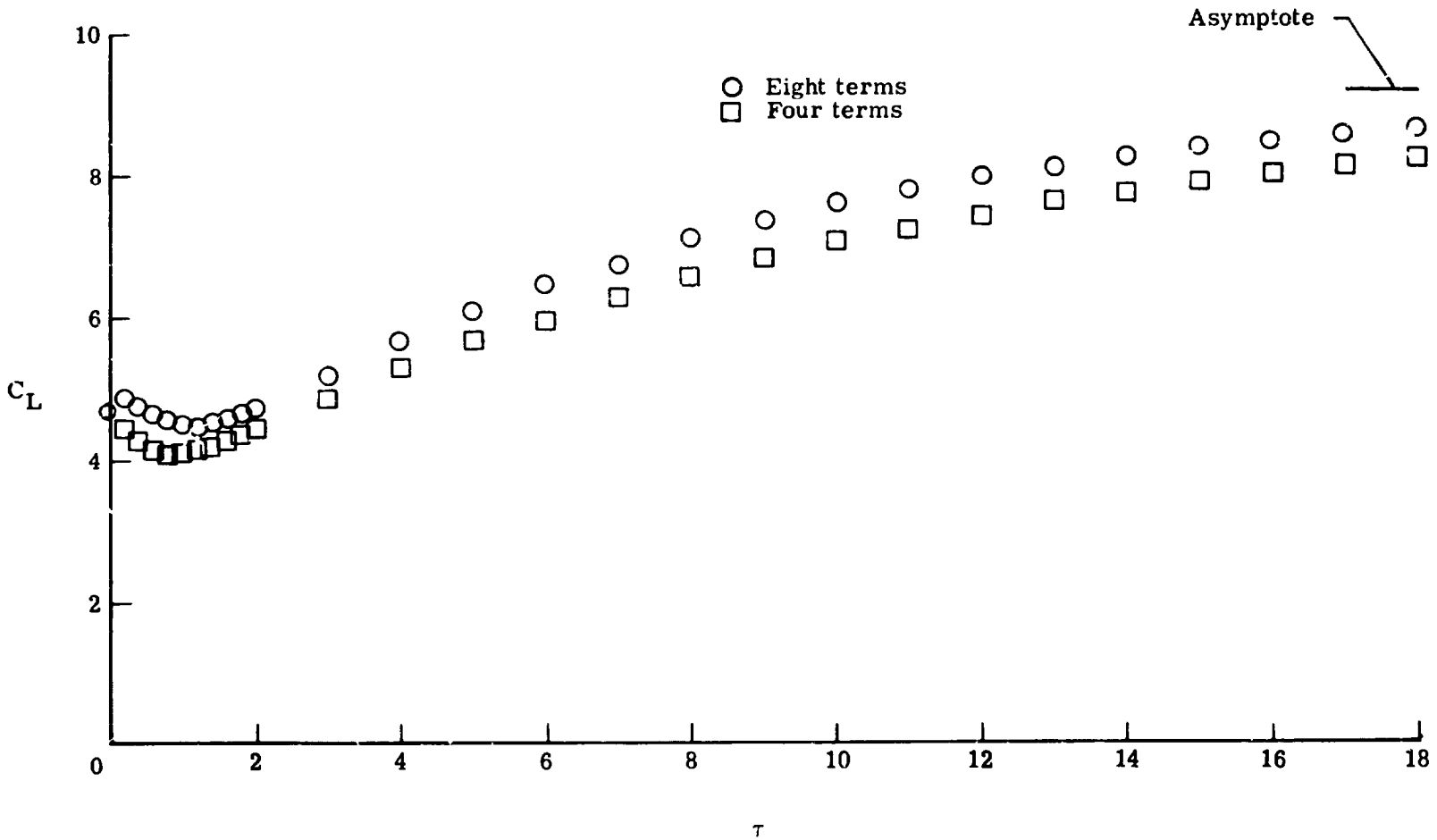

Figure 19.- Indicial lift due to step change in $\dot{h}/U$.

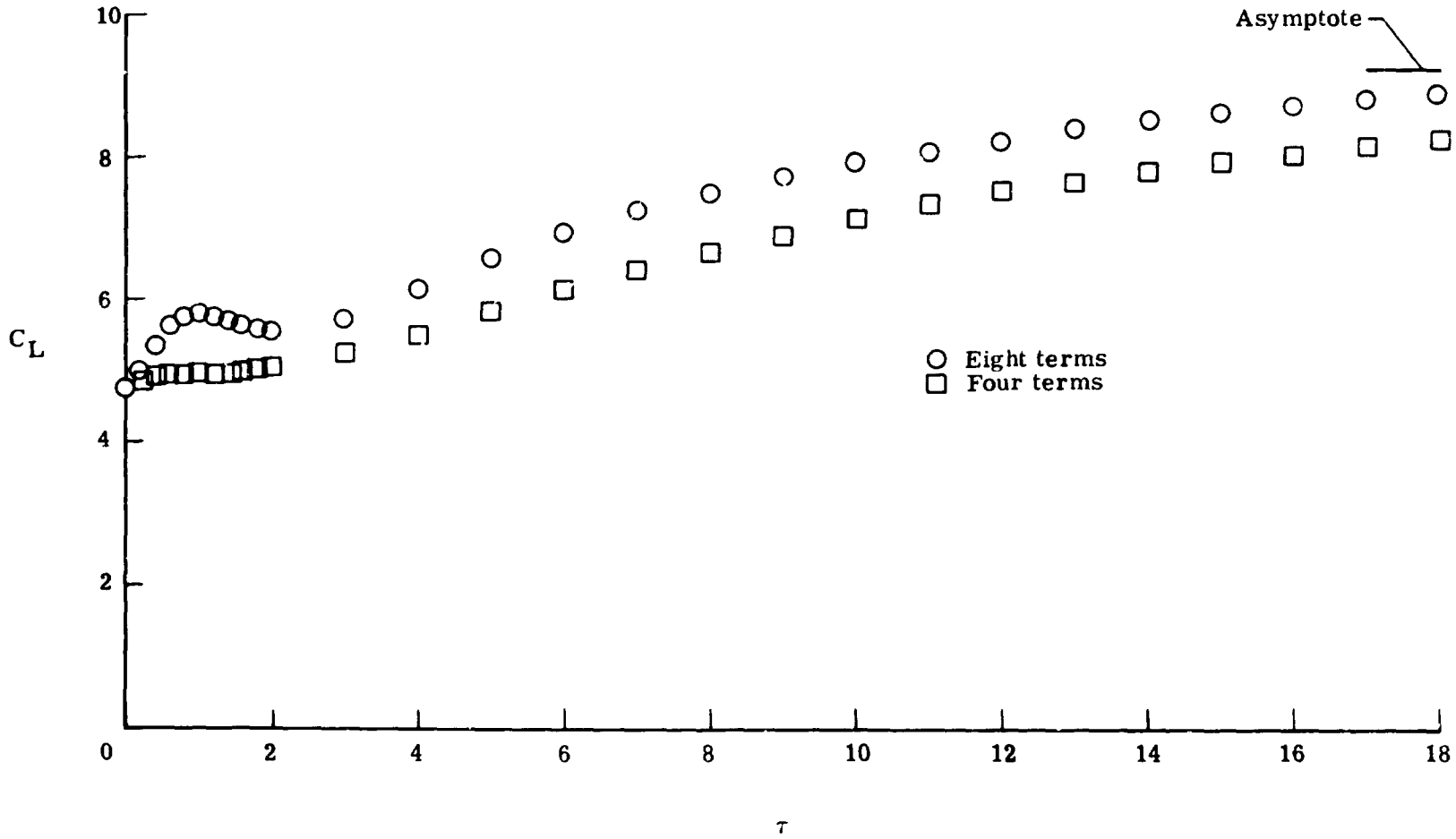

Figure 20.- Indicial lift due to step change in α.

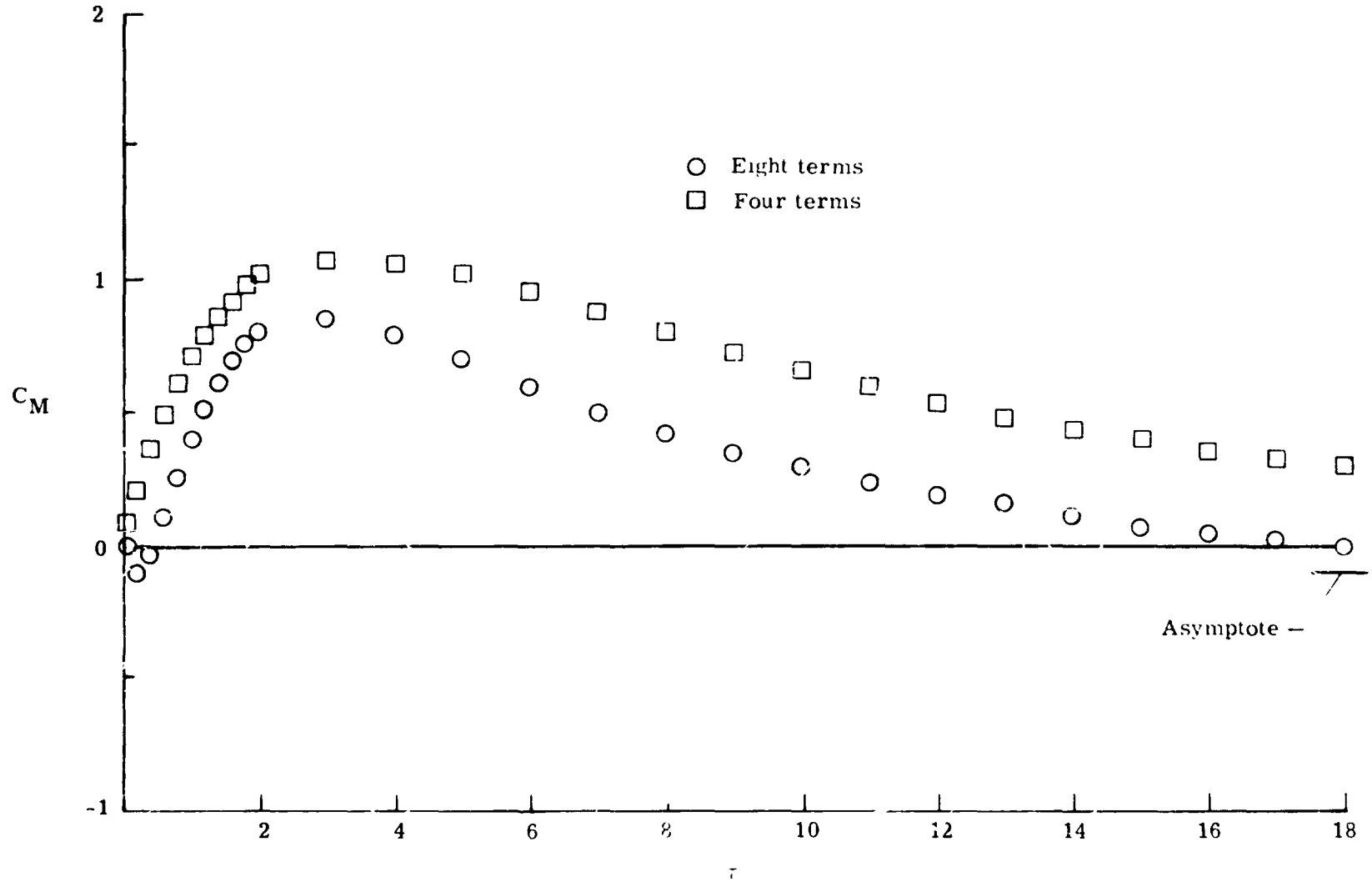

Figure 21.- Indicial moment due to step change in $\dot{h}/U$.

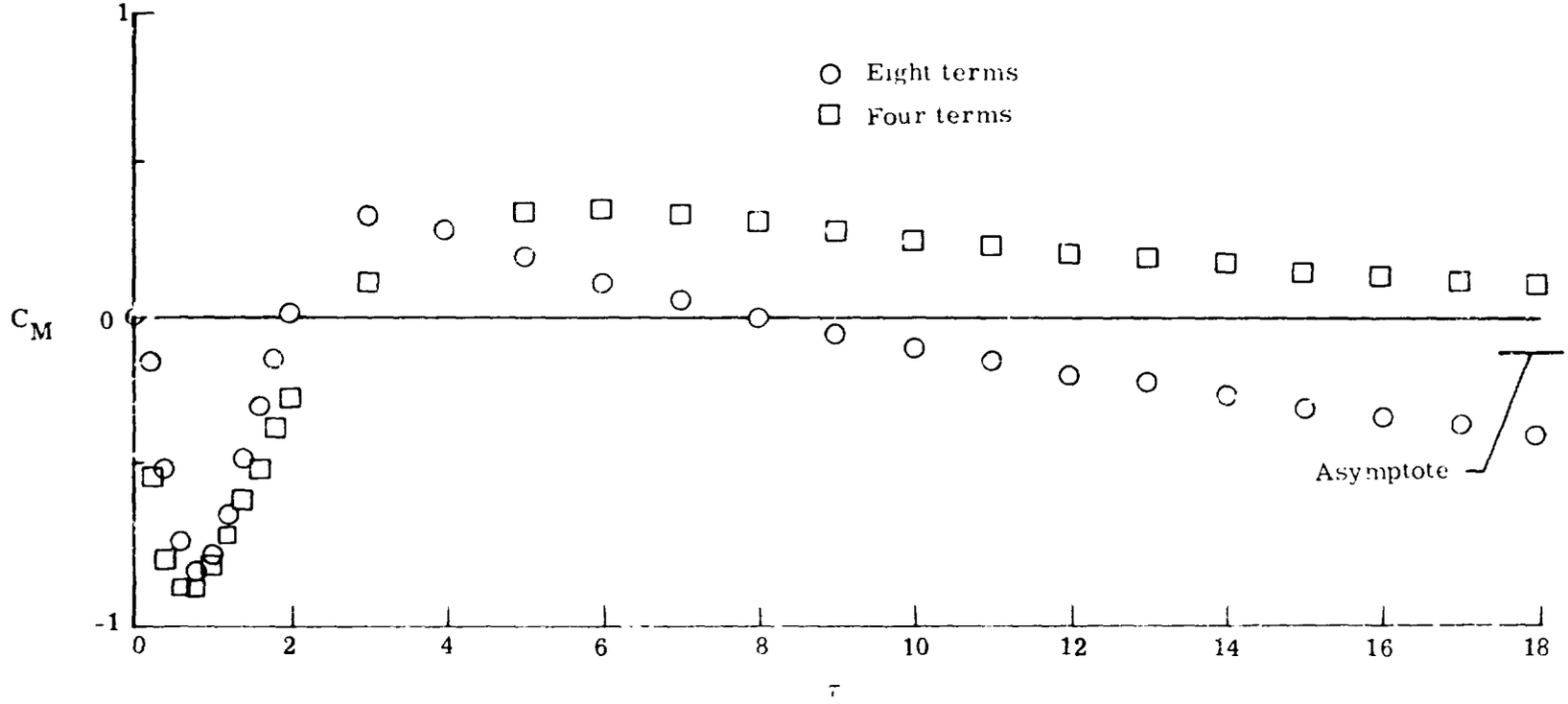

Figure 22.- Indicial moment due to step change in α.